A NOVEL JOINT INSPECTION METHODOLOGY BASED ON IMAGE ANALYSIS APPROACH FOR CONCRETE PAVEMENT CONSTRUCTION

A Thesis

by

RICHA BHARDWAJ

Submitted to the Office of Graduate and Professional Studies of
Texas A&M University
in partial fulfillment of the requirements for the degree of

MASTER OF SCIENCE

Chair of Committee,	Dan G. Zollinger
Committee Members,	Zachary Grasley
	Robert Lytton
	Reza G. Langari
Head of Department,	Robin Autenrieth

August 2018

Major Subject: Civil Engineering

ABSTRACT

Sealed sawcut joints are an essential feature of jointed concrete pavement construction and performance as they not only accommodate movements associated with concrete slabs but also prevent entry of moisture and incompressibles into the joint. Quality adhesion between sealant and concrete is critical for optimum performance of sealed joints. If present in significant amounts, contaminants like dirt and moisture on joint surfaces at the time of sealant installation adversely influence the sealant-concrete adhesion leading to premature failures. Presently, there are little or no definitive criteria for maximum tolerable contamination levels, which won't affect the durability of the adhesive bond between sealant and concrete. There is a need of critical construction items for engineers to specify and for inspectors to determine if a sawcut joint is sufficiently clean for sealant installation in order to reduce the frequency of debonding failures.

This research study aims at developing reliable surface assessments through the use of image analysis for different dirt levels on joint walls. Images of sawn concrete surfaces were analyzed through Image J software, which is able to capture changes in surface texture due to dirt accumulation in terms of surface height and area parameters. While dirt was quantified through imaging, moisture contamination was quantified with microwave technology. These indirect measurements of surface contamination were verified with tensile bond strength testing. Adhesion between sealant and concrete was studied at different contamination levels of dirt and moisture at different ages of concrete. Fresh concrete sealing and resealing cases were investigated separately, due to different boundary conditions for fresh sealant in both cases. Implications of this study involve the relation of these indirect measurement parameters with bond strength and specification criteria to govern the quality of sealant installation under field conditions.

DEDICATION

To my grandparents Brahmi and Ram Das,

my love and my strength

.

ACKNOWLEDGEMENTS

My sincerest appreciation and gratitude goes to my advisor Dr. Dan Zollinger, whose valuable counsel and continuous support helped me grow in both personal and professional spheres during the course of my Master's education. I would also like to thank Dr. Grasley for his guidance on not only technical matters but also on course of my career as a researcher. Special thanks to Dr. Robert Lytton and Dr. Reza Langari for serving on my committee and providing constructive inputs to this research.

I would also like to extend my thanks to my talented colleagues Jinho Kim, Dave Dillon, Patrick Moore and Seunghyun Lee, for their keen contributions to experimental portion of this research. I am grateful for all the wonderful friends and colleagues at Texas A&M University, who made this journey genuinely incredible and unforgettable.

Finally, I want to express my regards to my parents Ashwani and Anita, who have always shown faith in my every endeavor and my little sister Samiksha, who is a ray of sunshine to my heart. Last, but not least thanks to my dear friends back home, for always being an integral part of my life.

TABLE OF CONTENTS

Page

LIST OF FIGURES

LIST OF TABLES

CHAPTER I

INTRODUCTION

Transverse joints form a vital component of rigid pavement performance. These are designed to allow the pavement to expand and contract with environmental changes in temperature and humidity while maintaining its structural integrity. During their lifetime, jointed pavements experience various stresses which arise from the effect of the traffic loading, environmental conditions and material properties of the pavement layers. Joints are provided to accommodate regular slab movements and reducing the building up of climatically related pavement stresses. They control the location, width, and appearance of expected cracks and minimize the probability of unexpected ones. Figure 1 shows the types of joints based on their location on the slab.

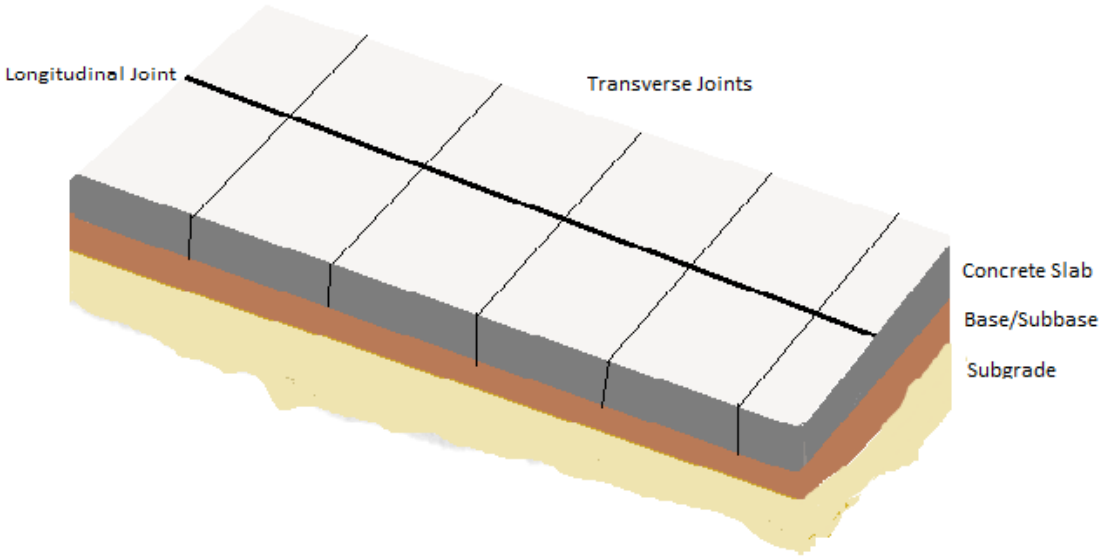

Figure 1 – Typical jointed plain concrete pavement

These joints are formed with sawcuts in the pavement surface and are sealed with different kinds of sealants, to prevent the accumulation of debris and water from infiltrating the joint and contributing to any distresses in the vicinity of the joint. Figure 2 shows a cross-section of a typical sealed joint. A sealed joint system consists of sealant and backer rod, acting as elastic filler materials to prevent joint and pavement from any contamination from water or incompressibles. Incompressibles are solids like dust and small rocks if allowed to accumulate in joints can restrict the expansion movement experienced by concrete slabs in hot environmental conditions.

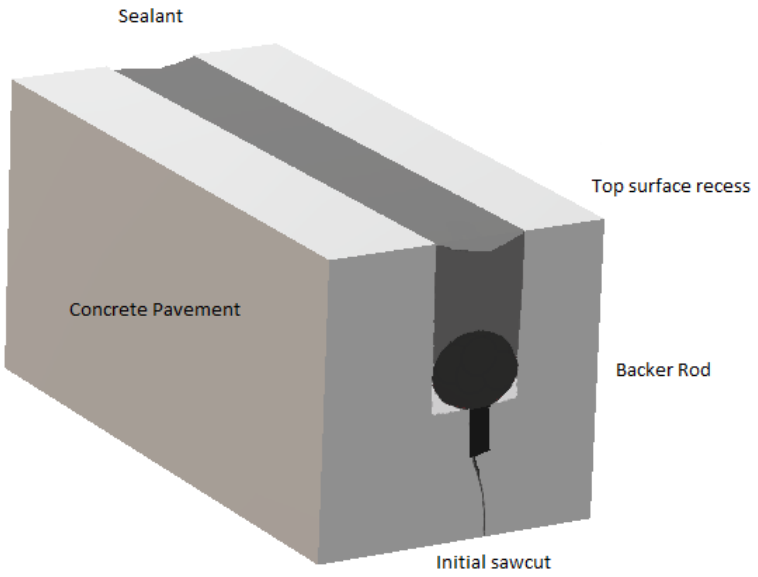

Figure 2 – Typical Joint Configuration

During its lifetime, a sealant experiences horizontal stresses due to shrinkage associated with early stages of hydration and thermal expansion and contraction of the slab. Both these movements are considered for calculating joint movement for new concrete pavement, while in case of resealing only thermal movement is considered. In winters, sealant experience tensile stresses due to

contraction of the concrete slab. On the other hand, compressive stresses are induced in sealant in summers, due to the expansion of the concrete slab. Minor stresses are also produced due to traffic loading and warping and curling of concrete slabs. Warping and curling stresses are produced in a concrete slab when there is a significant temperature gradient between top and bottom of the slab. Considering these joint movements, elongation properties of sealant are very critical to keep sealant bonded to the joint surface. Expected joint movement is calculated by the following formula [1] :

$\Delta L = C. L. (\alpha.\Delta T + \varepsilon)$

Where ΔL is change in length of the slab(in), L is the length of the concrete slab(in), C is base/slab frictional restraint factor, α is coefficient of thermal expansion of PCC, ΔT is maximum temperature range and ε is the shrinkage coefficient of the concrete.

A sealed joint is said to be failed if it is not preventing water infiltration into pavement substructure or is not able to accommodate the movements experienced by the slabs. Surface moisture can act as a carrier for deicing chemicals, which corrode steel rebars inside the pavement. The free water inside pavement can erode the finer particles of subgrade and transport these into the surrounding land. It can also lead to pumping of these finer particles out of the pavement cracks or joints if high hydraulic pressure develops inside the pavement. Pumping of finer particles can induce further cracking in the pavement if hydraulic pressure beneath the pavement becomes very high. Both these situations lead to weakening of support beneath the pavement, which may lead to faulting. Faulting is pavement distress in which joint walls have different elevations either due to loss of material beneath slab or due to construction error. Faulting exposes one face of the joint directly to oncoming traffic, which ultimately damages the concrete slab at that joint.

Another result of joint failure is the restricted movement of concrete slabs, which induce stresses in concrete near joint faces. If these stresses exceed the strength of concrete, pavement distresses like spalling, blow-ups, corner breaks and mid-panel cracks may occur. Spalling is pavement distress when concrete near joints is damaged, ruptured or torn apart. Corner break is cracking that initiates from the corner of the slab. Blowup is localized upward movement of the slab and shattering at joints or cracks. Mid panel cracks are transverse cracks that occur in the middle of the slab. All these distresses have accelerating effect on each other. Thus, adequate joint performance is essential for effective pavement performance, as joint failures are one of the main reasons behind the failure of jointed concrete pavements [2].

Sealant types and materials

Sealants are classified traditionally into three categories based on their physical state at the time of sealant installation in the field. These are namely hot pour sealants, cold pour sealants, and preformed sealants.

Hot pour sealants are first generation asphalt-based sealants, which are poured into joints at specific temperatures in the field. They may lose their properties if proper temperature control is not maintained.

Cold pour sealants are mainly silicone based sealants that do not need any mixing or temperature control for installation but need some curing to get into its final form. They are more costly but have shown greater service life than hot pour sealants. They are also better suited for wide temperature ranges.

Preformed sealants are neoprene based elastomeric seals that can be directly installed into joints. These are the most expensive ones. They are not bonded to the joint surface and are designed

to experience compression throughout their service life. Joint failure is abrupt as they tend to twist and move up and down when compression is lost.

Backer rods are provided in case of liquid sealants only. These are cylinders of compressible materials, which are at least 25% larger in diameter than the joint width. They are mostly made up of polyurethane, polyethylene, neoprene, etc. Backer rod ensures that sealant is not bonded to the bottom of the joint reservoir. Otherwise, excessive stresses are induced in the seal.

Sealant Performance

Joint seals mostly fail due to flawed design and faulty installation. Many construction factors like moisture and jet fuel are detrimental to the sealant, causing material deterioration. Primary factors that affect the quality of sealed joint systems are described as following:

1.) Joint Design: Along with joint width obtained from expected joint movement, it is critical to have an appropriate shape factor of sealant in the joint. Shape factor is depth to width ratio of sealant. It helps in minimizing the adhesive stresses and cohesive strains in sealants and optimizing sealant use. Generally, sealant manufacturers provide a range of recommended shape factors for different joint dimensions. An optimum shape factor ensures there is sufficient bond area to counter tensile stresses at the sealant-concrete interface so that strains in sealant due to expansion and contraction of joint don't lead to adhesive failure at this interface.

2.) Material Selection: For a specific application and climatic condition, sealant properties for long-term performance should be evaluated. These include resistance to jet fuel, compatibility with aggregates or backer rod, weatherability and durability. Elasticity and

modulus of sealant are also essential factors in considering sealants for specific climate types.

3.) Quality Installation: Proper sealant installation lead to the optimum development of adhesive strength between concrete and sealant. Quality installation means adequate joint surface preparation before sealant installation and maintenance of shape factor at the time of sealant installation.

Sealant Installation Practices

The sealed joint system is formed in the rigid pavements in following order:

1.) Sawcutting the joint into slab: Sawcutting is done in two successive steps. First cut is made within hours of slab construction while the concrete is hardening up to the point when it can withstand the shearing action of saw blades, without spalling. If concrete is too strong, deeper cuts are needed to control cracking. A second cut is generally made within seven days of curing, to properly shape the joint into its designed depth just right above the first cut. This second sawcut ensures that desired shape factor is achieved. The effectiveness of sawcutting also depends upon the coarse aggregates involved. It has been observed that crack control is least reliable for gravel aggregates. Generally, sawcut depth range from $1/3^{rd}$ to $1/4^{th}$ of the depth of the slab but these depths can be lesser in case of early-entry cuts. Saw blades are mostly diamond or carborundum tipped, to match the hardness of the coarse aggregate used in the concrete. Generally, harder aggregate concretes are cut with slower speeds.

2.) Surface Preparation: Joints need to be thoroughly cleaned after the final sawcutting to ensure backing rod and sealant are correctly installed. Sawcutting produces a significant amount of dirt in the form of slurry, which gets deposited in freshly cut joints. Cleaning

procedures include waterblasting, sandblasting, airblasting or combination of any two of them. Wire brushing is also used for cleaning but has lost popularity due to its ineffectiveness with narrower joints. After the cleaning, the joint is typically airblasted with hot compressed air and left to dry for 1-2 days till visible traces of moisture disappear. Drying is critical to ensure the presence of moisture does not prevent adhesion between concrete and sealant.

3.) Backer Rod Installation: After surface preparation is complete, backer rod material is inserted into the bottom of the joint reservoir. Backer rod also helps in controlling the shape factor of the sealant, along with acting like a tooling aid. After backer rod installation, the joint is ready for sealant application.

4.) Sealant Installation: Sealant is pumped through a nozzle sized for the width of the joint. Sealant surface is recessed $1/8^{th}$ to a $1/4^{th}$ inch below the riding surface by the mechanical tooling, to eliminate contact between sealant and tires.

Sealant Failure Modes

Adhesive failure and cohesive failure are two main modes of failure in sealed joints. This study focuses on adhesion between sealant and concrete, which depends heavily on the surface preparation of joints surfaces at the time of sealing. Other failure modes include incompressible intrusion in sealant material, extrusion of the seal out of joint, material loss, etc. These are explained below:

1. Adhesive Failure: This failure is a consequence of insufficient adhesion between concrete and sealant. Sealant-concrete adhesion depends upon concrete surface conditions at the time of sealant application. Adhesive failure occurs when sealant debonds with joint due

to excessive tensile stresses at the sealant-concrete interface. Debonding provides easy access of water into pavement substructure leading to loss of support beneath the pavement.

2. Cohesive Failure: This is a failure of sealant as a material when it is not able to keep itself together in the face of extreme tensile stresses. It results in local tearing or rupture of sealant itself, leaving joint exposed to intrusion by water and incompressibles.
3. Extrusion failure: This failure occurs when the sealant is not given enough recess into shape factor, and it protrudes above pavement surface. Traffic can either flatten the sealant onto the pavement or pull it out from joint causing damage to the seal.
4. Incompressible intrusion: This failure occurs when sealant material gets too soft and incompressible get deposited into the joint and develop stresses along the joint wall surface.

PROBLEM STATEMENT

The effectiveness of the joint sealant to safeguard the pavement depends heavily upon the quality of installation and capability of sealant to adhere to the surface of the joint wall. This study deals explicitly with the adhesion effectiveness of silicone-based sealants only. There are two main surface contaminants – dirt and moisture, which act as physical barriers between a sealant and the wall of a concrete joint well preventing full adhesion. Despite various joint preparation methods including water blasting and hot-air blasting, some residual quantity of these contaminants may remain on joint surfaces at the time of sealant installation.

Methods of joint inspection prior to the sealant application include procedures such as wiping by a black cloth and visual inspection, but these are quite subjective in their application. An effective field inspection methodology should be able to meet following criteria:

1.) It should be portable with medium cost.

2.) It should be non-destructive, with the ability to produce the quantifiable surface assessment.

3.) It should be able to cover large areas in small time.

4.) Data acquisition and processing should be easy and fast.

5.) It should be applicable to all joint widths.

6.) It should be able to produce repeatable measurements.

Various studies have been done in the past to improve the sealant installation procedures by increasing quality control of joint surfaces. However, these studies have yet to deliver a universally accepted technique to quantify joint surface conditions. Therefore, there is a need for effective joint inspection method which can produce reliable surface assessments quantifying these residual contaminants to better support quality control decisions in the field.

OBJECTIVES

The purpose of this study is to develop a field inspection technique for indirect measurement of surface contaminants, along with understanding the development of sealant-concrete adhesion at different levels of contamination. The detailed objectives are explained below:

1.) To develop a field inspection method to quantify the surface characteristics of the joint well surface, that can produce objective, reliable data for creation of the database.

2.) To develop a relationship between the observed roughness values of the joint well surface and bond strength between the sealant and concrete surface.

3.) To understand the effect of surface moisture on the adhesion between the sealant and concrete surface.

4.) To understand the combined effect of moisture and dirt on the concrete surface on the development of adhesion between the sealant and concrete surface.

5.) To understand the difference between the moisture conditions at joint surface and distinguish between the development of adhesion between the sealant and concrete surface for cases of fresh concrete sealing and resealing.

RESEARCH SCOPE AND METHODOLOGY

This thesis aims at developing field inspection methodology for monitoring these surface contaminants, along with a better understanding of effects of these contaminants on sealant-concrete adhesion. The first part of this research presents a set of surface descriptors for describing joint well surfaces through a photogrammetric method. Sawn concrete have an inherently rough texture with depressions and protrusions on the surface. Any addition of dirt fills these depressions leads to a smoother surface. Thus, clean sawn surfaces have higher roughness than dirty ones. Images of sawn concrete surfaces in both clean and dirty states were analyzed through the use of Image J software to produce various roughness parameters as output. These parameters showed a significant decrease with the addition of dirt. The sensitivity of these parameters can be used to distinguish between clean and dirty joint surfaces in the field, with the help of a joint inspection device. One of the primary objectives of this study was to develop field inspection methodology for joint surfaces at the time of sealant installation. It was observed that image analysis approach

could produce quantifiable results in terms of roughness parameters, which gives it added advantage over other methods in creating sufficient data along a joint surface ranging between clean and dry states.

The final part of this research is focused on understanding the effect of dirt, moisture, and hydration on the development of the adhesive bond between sealant and concrete. This was done by analyzing silicone sealant-concrete adhesion by preparing concrete samples bonded with sealant and testing them till failure by application of tensile deformation as per ASTM D 5893 [3]. Silicone-based sealant Dow888 was used in this research for adhesion testing. Concrete samples were maintained at specific dirt and moisture levels at the time of sealing. Dirt was quantified through image analysis, while microwave technology was used to quantify moisture. Fresh concrete sealing and resealing were studied separately due to differences in porosity of these cases. The final aim of this study was to understand the impact of these variables on quality of sealant-concrete adhesion for further development of methodology and technology for indirect measurement of dirt and moisture in the field for adequate quality control at the time of sealant installation.

This research work is presented in five chapters in this thesis. Chapter 2 describes the literature review of studies that have researched related topics of sealant-concrete behavior. Chapter 3 includes the preliminary testing on image analysis methodology and its application in the field. Chapter 4 details the experimental study of sealant- concrete adhesion with respect to surface contaminants like dirt and moisture. Chapter 5 summarizes this thesis with conclusions and future recommendations

CHAPTER II

LITERATURE REVIEW

There are several types of transverse joints namely- construction, isolation, expansion and contraction joints. The transverse joint is joint provided in a transverse direction to the direction of traffic. However, this study is focused only on sawcut transverse contraction joints, which are provided at the time of pavement construction to control cracking. Expansion joints are traditionally provided in long panels (> 60ft), when there is the possibility of substantial expansion due to specific materials or due to low-temperature conditions at the time of pavement construction. Generally, if transverse joints are provided at strategic locations, there is no need of expansion joints.

In the early part of the 20th century, joints were wider, were often tooled rather than sawcut and were sealed with materials like wood, tar, or asphalt, etc. Also, cleaning practices were inadequate including brooming, leading to dirty surfaces getting sealed. Over the time, narrower sawcut joints with improved sealant materials became available yielding better performance. With narrower joints, the importance of joint reservoir design and shape factor was realized [4].Joint sealing is not effective in some cases, and thus there are some factors that need to be considered before sealing:

1.) Traffic levels
2.) Soil and Subbase use
3.) Amount of rainfall
4.) Pavement Type

Studies have suggested that joints can be left unsealed in hot and dry climates with low traffic levels [5]. Despite the doubts over the whether to seal or not, many states have adopted the practice

of joint sealing and have reported better pavement performance. Studies have reported adhesion failure to be the most common cause of sealant failure and can start as early as 1.5 years after installation [6]. Adhesion failure can accelerate pavement damage as debonded seals can provide passage of water and incompressibles into pavement substructure.

There have been various field studies to evaluate the long-term performance of sealants in the field. Cohesive failure is more common in case of hot pour sealants, while silicone based sealant mostly fails due to adhesive failure [7]. An inspection study of jointed pavements in Ohio, by Hawkins et al., showed that sandblasted joints have lower rates of full depth adhesion failure than ones with only waterblasting and airblasting [8]. Silicone sealants exhibit better resistance to aging and temperature changes and are easier for installation. Despite that, one of the main reasons behind poor sealant performance is poor workmanship at the time of installation [9]. A study by Ohio Department of Transportation implied that adhesion loss due to inadequate cleaning is one of the significant factors adversely affecting sealant performance [10].

Various laboratory studies have pointed out superior performance of silicone sealants, as they possess better bonding and expansion characteristics [11].ASTM C719 standardizes a cyclic loading test to evaluate sealant behavior but does not provide any criteria for sealant adhesion [12]. Al-Qadi et al. (1989) developed a new method to analyze sealant performance by applying a combination of constant horizontal and cyclic shear deformations, till 20% of sealant exhibit cohesive or adhesive failure. However, this study doesn't deal with adhesive strength specifically [13]. Still, due to a large number of variables involved, none of these studies are comprehensive enough for accurate prediction of field performance.

There have been attempts to develop a field applicable method for assessing the compatibility of concrete surfaces and sealants at the time of construction. ASTM C 794 describes

an adhesion-in-peel test to evaluate adhesion between concrete and sealant but is not that much reliable as testing involve pulling a fabric embedded in sealant rather than sealant itself [14]. ASTM C1521 describes non-destructive and destructive testing methods for identifying areas of poor adhesion in already sealed joints. Based on the results, specific joint preparation techniques may be suggested for rapid optimum adhesion between sealant and joint. If failure exceeds design parameters, evaluation of total joint movement may be needed. However, non-destructive methods of applying pressure on the seal with a dowel shaped tool or a wheel can cause destructive damage and are not recommended for high-temperature conditions. Destructive methods involve hand pulling a cut portion of sealant till failure, thus are highly subjective [15].

Due to vertical configuration and narrow width of joint, it has proved to be difficult to accurately measure the surface moisture at joint surfaces to be sealed. ASTM standardizes some methods for indirect measurement of moisture on concrete surfaces. These include techniques like plastic sheet test (ASTM D4263) and calcium carbide test (ASTM F 1869). However, both of them are long duration tests which require large surface areas, rendering them impractical for field application [16-17]

Other tests include relative humidity test, resistivity probe test, and radiometer test, which are nondestructive in nature. Relative humidity test is more adaptable to the joint configuration but is highly susceptible to air conditions surrounding the joint. Typically in the field, visual inspection is carried out after allowing a significant drying period of 1 to 3 days. It is recommended to apply sealant only when ambient temperatures are above the dew point, which is a temperature below at which air moisture condenses at joint surfaces and concrete show significant moisture absorption. Optimum drying period for joints also depends upon their width, as evaporation rates are lower for narrow joints. FHWA suggests another round of sandblasting and airblasting after drying if rain

or dew contaminates the joint surfaces [18]. Still, moisture act as one of the major contaminants preventing sealant concrete adhesion as careful visual inspection can only detect surface moisture without any quantification.

A study by WJE associates suggested these four tests: Moisture paper test, Wipe test, Tape contamination test, and the Tape pull test. First, three of them are subjective, and the last one is not reliable as the tape itself is susceptible to deformation or breakage. Moisture paper test can identify pockets of free water on the concrete surface but is not applicable to moisture present inside the concrete. Wipe test and Tape contamination test uses dark colored cloth and tape respectively for detection of dirt by wiping on the concrete surface of the joint wall. Tape pull-off test is based on ASTM D3359 standard for measuring adhesion by tape test. A set up for Tape test is shown in Figure 3.WJE associates also conducted tape pull off tests with various moisture and dust combinations, but the combination of dust and moisture was showing increased bond strength [19].

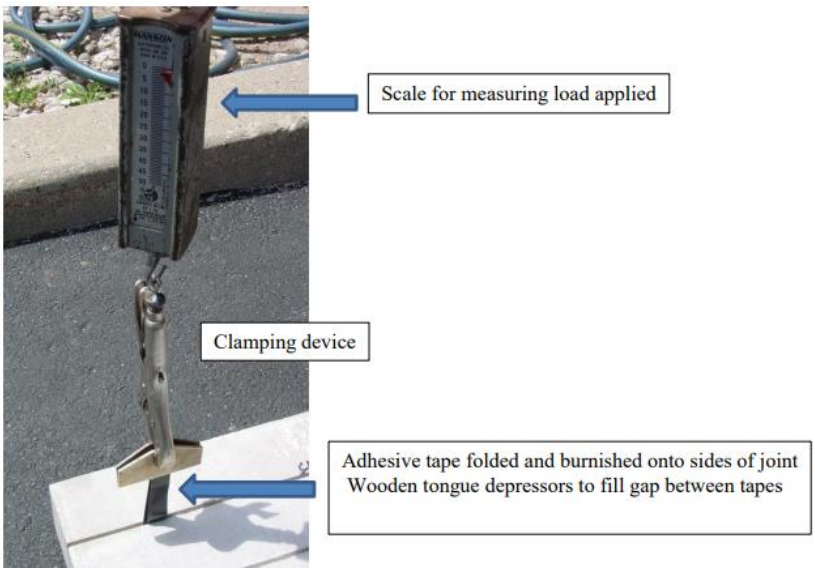

Figure 3 – Tape adhesion pull-off testing setup (Reprinted from [19])

Another test method developed by Qiang Li et al. (2014) tried to determine the effect of initial surface moisture conditions on the adhesive strength of concrete - silicone sealant samples. The study indicated a threshold value of surface moisture below which adhesive strength was not sensitive to surface moisture. Indirect measurement of moisture on the concrete surface was done with humidimeter, giving 80% RH as the threshold value. Humidimeter was employed as a surface probe taking measurements by placing the probe in contact with the concrete surface. However, this device needs metal inserts inside concrete for accurate measurement and is not recommended for fresh concrete. Dry concrete specimens showed highest adhesive strength, while specimens in wet condition have significantly reduced strength. Still, this study did not accommodate dirt and moisture combinations.

An extension of this research was developing a field test which measures adhesive strength by applying a tensile deformation to concrete specimens glued with cylindrical sealant bead, but this method is time-consuming and uses a repro-rubber compound rather than actual sealant itself [20]. Figure 4 shows the joint inspection device as inserted in a joint.

Figure 4 – Joint Inspection device (Reprinted from [20])

A force multiplier was used to measure the force needed to pull out the repro-rubber compound entirely out of joint. Results didn't show any clear distinction between joints at different dirt and moisture states.

Joint walls being near the top surface of pavement, experience significant temperature gradients with time, with maximum temperature in the afternoon and minimum temperature in the morning. These, in turn, affect evaporation rates of moisture present in top part of the concrete slab, leading to high capillary tensions. These evaporation rates depend upon the age of concrete, porosity and temperature gradients [21]. This points to a case where some moisture is tolerable as high capillary tensions can pull some of the moisture inside the concrete substrate away from sealant concrete interface. These threshold values of allowable moisture contamination should be significantly different for fresh concrete sealing and aged concrete sealing case, due to following reasons:

1.) There is considerable drying shrinkage at the top surface of the pavement near silicone sealant. 20% to 30% of which occur in first 2 weeks, when the sealant is applied and not fully hardened yet [21]. In case of freshly sawcut concrete, some of the surface moisture can be utilized for offsetting the drying shrinkage ultimately becoming a part of the concrete microstructure.

2.) Porosity involved in both cases is different. For this particular concrete mix design with w/c of 0.45, capillary porosity was 0.0972 cm3/g, and the gel-space ratio was 0.8832 when hydration was 99% complete as calculated by Powers model [22]. At the time of 7 days assuming 65% hydration, capillary porosity was 0.216 cm3/g and gel-space ratio 0.671.

Such huge differences in porosity will lead to different moisture diffusivities and capillary tensions in concrete samples. Relative humidity profiles for concretes at various stages of curing are shown in Figure 5.

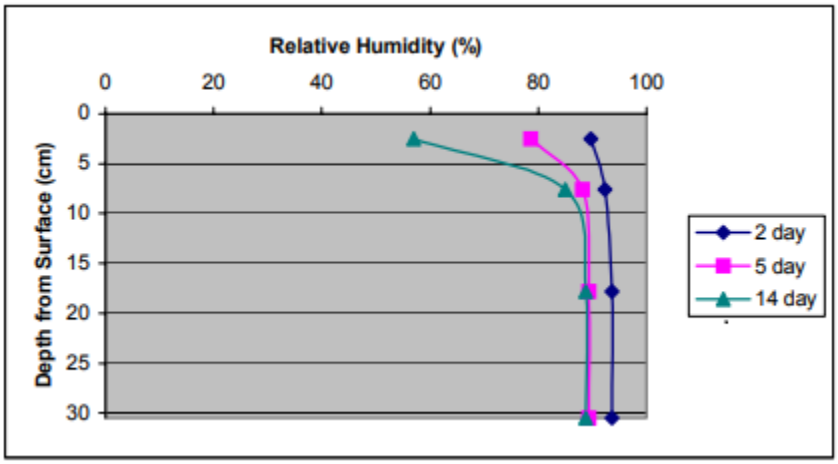

Figure 5 - RH profiles of concrete vs. stages of hydration

As hydration progresses, there is a shift in relative humidity profile over the time. These changes will manifest themselves in the form of evaporation rates and moisture migration. Thus, the age of concrete and porosity needed to be considered in determining the threshold for surface moisture. There is a requirement for a reliable method of surface assessment of joint surface to check the quality of surface preparation at the time of sealant installation. Various fields like biology, medicine, construction, paper technology, etc. require reliable surface representations in terms of roughness parameters. Roughness quantification has been used by concrete researchers for its usefulness in understanding the role of surface roughness in the behavior of concrete to concrete interfaces. Quantification of surface characteristics can be achieved through several techniques including stylus profilometers, atomic force microscopy, scanning electron microscopy, laser

profilometry, etc. These methods are able to provide with reliable surface representations, but are high ended complicated and expensive. It is difficult to translate these technologies into non-destructive technologies for real-time data acquisition and processing of joint surface characteristics in the field [23]. Table 1 provides a comparison of various roughness techniques used for surface characterization of concrete surfaces.

Table 1 Comparison of surface characterization techniques for concrete surfaces

Method	Quantification	Non-Destructive	Cost	Portability	Work Intensive	Surface Contact
Concrete Surface Profiles	No	Yes	Low	Yes	No	No
Sand Patch Test	Yes	Yes	Low	Yes	No	Yes
Outflow Meter	Yes	Yes	Low	Yes	No	Yes
Mechanical Stylus	Yes	No	Medium	No	Yes	Yes
Circular Track Meter	Yes	Yes	Medium	Yes	No	No
Digital Surface Roughness Meter	Yes	Yes	Medium	Yes	No	No
Microscopy	Yes	No	High	No	Yes	No
Ultrasonic method	No	Yes	Medium	Yes	No	No
Slit-Island Method	Yes	No	Low	No	Yes	Yes
Roughness Gradient Method	Yes	No	Low	No	Yes	Yes
Photogrammetry	Yes	Yes	Medium	Yes	Yes	No
Shadow Profilometry	Yes	Yes	Low	Yes	Yes	Yes
Air Leakage Method	No	Yes	Low	Yes	No	Yes
PDI Method	Yes	No	Low	No	Yes	Yes
2D-LRA Method	Yes	Yes	Medium	Yes	No	No
3D Laser Scanning	Yes	Yes	High	Yes	No	No

Image data of the surface can be analyzed to get roughness and cleanliness of surface which is a good indicator of its adhesion potential with other substances. The surface roughness doesn't only depend upon joint preparation methods, but also on the age of material and workmanship of technicians involved [23]. Application of image analysis in concrete research began with detection of surface entities like micro-cracks. Some studies utilize fluorescent dye techniques to highlight a surface feature to be identified, which is useful in case when only one type of defect is of interest [24]. Researchers are employing image analysis for characterization of plastic shrinkage cracking in fiber reinforced concrete [25]. This has been extended to the characterization of aggregates, microspores, later to be employed in micromechanical modeling [26].

This paper reports on the employment of image analysis approach as a reliable surface assessment of the transverse joints in concrete pavement. Images are examined through the Image J software to get image roughness parameters. Image J software has been preferred by the concrete researchers, due to its easy accessibility, and extensible platform for 2D and 3D image processing and analysis [27]. However, the main use of Image J in concrete research has been determining pore structure and permeability of concrete by examining stacks of images from X-Ray tomography techniques and microscopy. Image J software has also been utilized in assessing damage by alkali-aggregate reaction in concrete structures [28]. Quality control of decorative horizontal surfaces can be evaluated by introducing tolerances for surfaces blemishes [29].

The roughness quantification is performed by Surf char plugin of Image J software. This plugin was developed for surface characterization of calendared paper coated with mineral fillers like gold and carbon. This plugin is based on gradient analysis for ensuring intensity and orientation of surface structures. Surface descriptors like roughness and surface area were developed to quantify the surfaces in terms of coverage by mineral fillers. The efficiency of surface

descriptors for reliable surface assessment of paper was verified with results from laser profilometry and scanning electron microscopy [30].

Summary

There is no reliable objective joint inspection methodology in practice, which can produce quantifiable data regarding surface characteristics of the joint well at the time of sealant installation. This lack of database is an impediment to further research in improving the long-term performance of sealant-joint systems in the field. The subjective and raw nature of surface assessment at the time of sealant installation leads to insufficient cleaning and drying of joint wall surfaces. One of the main reasons behind premature failures of silicone sealants in the field is this inadequate joint surface preparation, leaving a considerable amount of surface contaminants on the joint surface.

The effect of surface moisture on the development of sealant concrete adhesion has not been researched extensively. There is lack of significant experimental data on resultant adhesion when both dirt and moisture are present significantly in at the same time.

The distinction between fresh concrete sealing and resealing is not established in previous research studies about the effect of moisture on bond strength. Initial sealing involves sawing fresh concrete with hydration still going on, while concrete surface in resealing is completely hydrated. Surface moisture in both cases cannot be treated as same, as fresh concrete is actively consuming moisture for further hydration.

It is crucial to separately analyze and characterize concrete surfaces of the joint well interface and tie down this characterization to sealant performance in the laboratory, in order to accurately assess and predict sealed joint performance in the field. This study focuses on developing reliable surface assessment technique for quality control of joint well surfaces at the

sealant installation. These surface assessments should be able to reflect the quantity of surface contaminants on the concrete surface to be sealed. Therefore for adequate quality control in the field, it is very critical to study the effect of surface contaminants on the sealant concrete adhesion and develop relationships between surface assessments and sealant concrete adhesion.

CHAPTER III

IMAGE ANALYSIS METHODOLOGY

An ideal joint inspection method should be non-destructive with low operating cost and should be able to overcome the narrow size limits associated with joint configuration in the field. Photogrammetric methods often have the edge over other nondestructive methods due to the easy and fast application with medium costs. Also, images can be stored for further processing and data analysis in future, generating a database.

This research study is focused on developing a new approach for joint inspection based on image analysis to characterize sawn concrete surface, in order to establish threshold values of minimum acceptable dirtiness levels at the time of sealant installation. This is achieved by analyzing images of different sawn surfaces through the use of Image J software and quantifying surfaces through various parameters like roughness, profile height, skewness, and kurtosis. These parameters show marked decrease with increase in dirtiness. This inverse relationship between Image J parameters and dirt is studied for varying levels of dirt on different sawn concrete surfaces. Real-time inspection is possible with endoscopic cameras having wireless capabilities that ensure instant transfer of images to a computing system.

Apart from joint inspection, this research also studies the effect of dirt, moisture, and hydration on the development of the adhesive bond between concrete and sealant. Image analysis parameters were verified with the tensile bond testing of sawn concrete samples sealed with silicone based sealant. Sample preparation included varying dirt and moisture levels to develop a relationship between Image J surface descriptors and the adhesive strength between concrete and sealant as measured by tensile bond strength testing.

ASSEMBLY FOR JOINT INSPECTION

A joint inspection device for this work was manufactured to accommodate the endoscope camera. Other components of joint inspection device include inserts with mirror, a holder for the camera and inserts to take images of sawn concrete surfaces along the narrow joints as shown in Figure 3. Mirrored inserts were machined to different sizes so that the assembly can fit in a 1/8th inch, 1/4th inch, 1/2nd inch and 3/8th-inch joints. The camera can be connected to an android phone or a laptop to obtain images or video of the sawn concrete surfaces in real time. Mirrored inserts are angled at 45^{o}, so that reflection of vertical concrete walls of joints is obtained on the mirror. The endoscopic camera captures the image of this reflection and transfers it to the processing system. This device only images one vertical wall of joint facing the mirrored insert, in one continuous run. Thus for complete inspection of both the vertical walls of the joint, two runs in opposite directions are needed. The working of joint inspection device is explained in Figure 6.

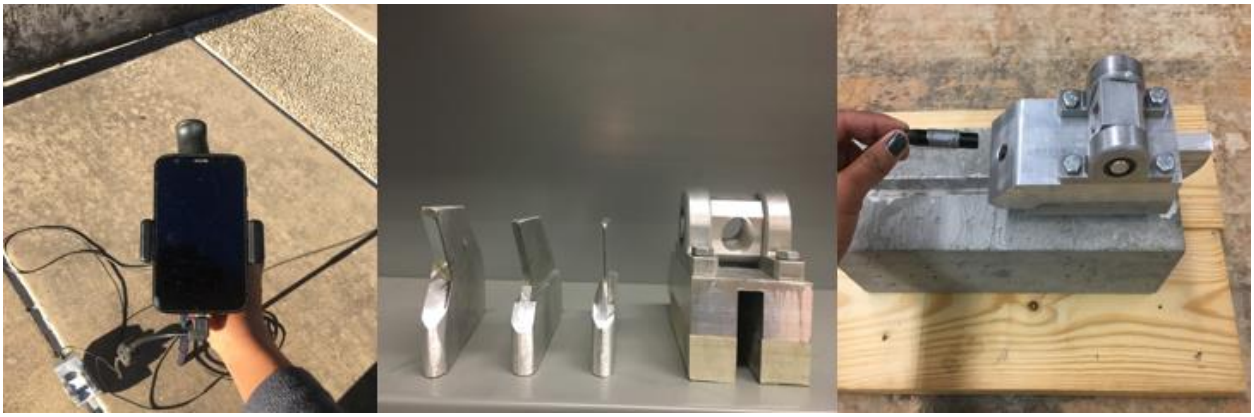

Figure 6- Joint inspection assembly

SURFACE CHARACTERIZATION THROUGH IMAGE J SOFTWARE

A good quality image is necessary for reliable assessment in terms of different surface parameters. The terminology of surface roughness examination through image analysis revolves around the z pixel values or height of the profile. Peaks are surface protrusions above the datum plane, while valleys are depressions on the surface below the datum plane, described below, as shown in Figure 7.

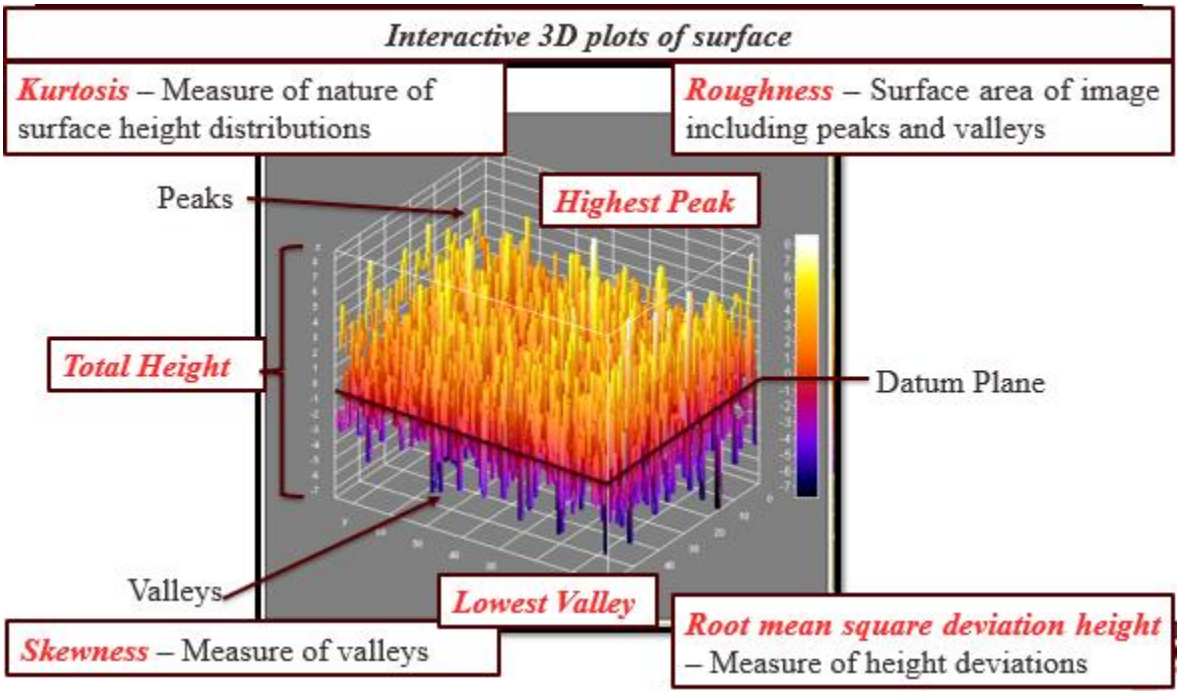

Figure 7 - Main features of 3D plot obtained through Image J software

This study utilizes SurfChar plugin of Image J software [31]. Plugins are additional components to software, that are not integral part of software but can be added later to extend the functionality. SurfChar plugin was developed for the study of the surface texture of calendared paper as explained in Chapter 2. At first, the image is subjected to Fast Fourier Transform, which is used

when geometric characteristics of the image are to be analyzed. Fourier transform makes the data analysis easy by decomposing image data into its sinusoidal components.

The SurfCharJ plugin calculates roughness parameters (elaborated below) in pixels through local roughness analysis, according to the ISO4287/2000 standard [32]. The z pixel value is the vertical distance to the surface, while x and y pixel values are coordinates of datum surface. SurfChar plugin produces a variety of roughness parameters, but only a few of them are relevant to this study. Since these values are in pixels, they need to be converted into desired units by dividing by the previously noted conversion factor. Calibration of the image is done using a standard image to get the image parameters in μm rather than pixels. The conversion factor depends upon focal length and resolution of the camera.

Main parameters used in this analysis are:

1.) Average Height (R_a): It is the arithmetic average of the absolute values of profile heights over the evaluated area and above the datum surface. This is based on light scattered by the surface and given by following formula in pixels:

$$Ra = \frac{1}{N_x N_y} \sum_{i=1}^{N_x} \sum_{j=1}^{N_y} | z_{ij} |$$

Where N_x and N_y denote the number of discrete measurements in x and y direction respectively and z_{ij} is the amplitude of each measurement.

2.) Root mean square deviation height (R_q): It is the average of the measured height deviations taken within the evaluated area. R_q is more sensitive to peaks and valleys than R_a and is given by following formula in pixels :

$$R_q = \left(\frac{1}{N_x N_y} \sum_{i=1}^{N_x} \sum_{j=1}^{N_y} {z_{ij}}^2 \right)^{1/2}$$

3.) Skewness (R_{sk}): It is the measure of the asymmetry of the surface with respect to a datum surface. Negative skew values indicate that surface has most of its profile below the mean line, which indicates more valleys or depressions on the evaluated surface.

$$R_{sk} = \frac{1}{{R_q}^3} \frac{1}{N_x N_y} \sum_{i=1}^{N_x} \sum_{j=1}^{N_y} {z_{ij}}^3$$

4.) Kurtosis (R_{ku}): It is used to measure the peak of the distribution of the intensity values around the mean. High values of kurtosis indicate z pixel distributions with sharp peaks and long fat tails, while low values are generally associated with rounded distributions and shorter thin tails. Low values of kurtosis are typical with uniform and regular surface features.

$$R_{ku} = \frac{1}{{R_q}^4} \frac{1}{N_x N_y} \sum_{i=1}^{N_x} \sum_{j=1}^{N_y} {z_{ij}}^4$$

5.) Total height (R_t): It is vertical distance between maximum peak height and maximum valley depth for a given sampling length. This parameter is calculated in pixels and is given by following formula :

$$R_t = \frac{1}{N_x N_y} \sum_{i=1}^{N_x} \sum_{j=1}^{N_y} (p_i + v_i)$$

where N_x and N_y denote the number of discrete measurements in x and y direction respectively. p_i and v_i are peak height and valley depth respectively in each sampling length.

6.) Surface Area (S_A): It expresses the increment of the interfacial surface area relative to the area of the projected (flat) datum plane. A rougher surface will have higher surface area than a smooth surface. This parameter is represented in calibrated units and is given by following formula:

$$S_A = \iint \sqrt{1 + \left(\frac{dz}{dx}\right)^2 + \left(\frac{dz}{dy}\right)^2}\, dxdy$$

Surf char plugin evaluates all these parameters locally over different sampling lengths to ensure local variation is well reflected in these parameters.

IMAGE ACQUISITION AND PROCESSING

The joint inspection device is inserted inside a saw cut. The joint face is photographed using the endoscopic camera, from where images are directly acquired and transferred to a desktop system with the Wi-Fi feature of the endoscopic camera. These images are analyzed with the help of Image J software to obtain output in terms of roughness parameters. Each image represents the different surface texture of the concrete at a specific location of joint. Since clean and dirty concrete surfaces have different surface roughness as discussed in Chapter 1, the value of these roughness parameters obtained from Image J software is significantly different for these surfaces. Image J can process multiple images simultaneously in the form of stacks, to give a table of roughness parameters for

a specific case.

The roughness analysis is performed through Image J software in following steps:

1.) Procured images are cropped through Image J software to get required image size in the form of stacks.
2.) The colored images are converted to 32 bit black and white images, as SurfChar plugin only analyze this format of images.
3.) Images are first subjected to Fast Fourier Transform plugin.
4.) Images are then subjected to SurfChar plugin.
5.) Output comes in the form of a table containing all roughness parameters.
6.) Parameters of interest as explained below are converted into normalized units.
7.) The last step involves getting an interactive 3D plot by subjecting the processed image through the 3D plugin of Image J software.

Normalization of parameters

Image J parameters like R_q, R_t, and S_A were normalized with a standard smooth surface having following values of these parameters as shown in Table 2.

Table 2 – Image J parameters from standard surface

R_q	R_t	S_A
750µm	4800µm	195000µm^2

The parameters were normalized to get unitless values in the range of 0 to 100 so that output from Image J can be easily interpreted.

PRELIMINARY IMAGE ANALYSIS

Preliminary image analysis was conducted to check the ability of Image J parameters in differentiating surfaces having visibly different textures. The surfaces studied were polished wood, sawcut concrete, pavement surface and expanded shale. Figure 8 shows the surfaces with different surface characteristics.

Figure 8 – Visible texture of different surfaces

Image J parameter R_t which signifies total height of profile measured from surface depressions, increased significantly with increasing visual roughness as shown in Figure 9.

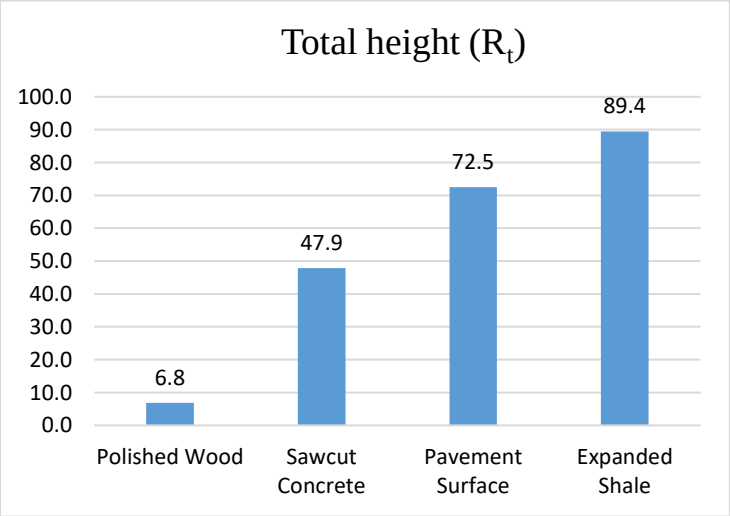

Figure 9 – R_t parameter for different surfaces

Similarly, R_q parameter signifying the deviation of surface height values from a mean height, showed a considerable increase with the increasing roughness as shown in Figure 10.

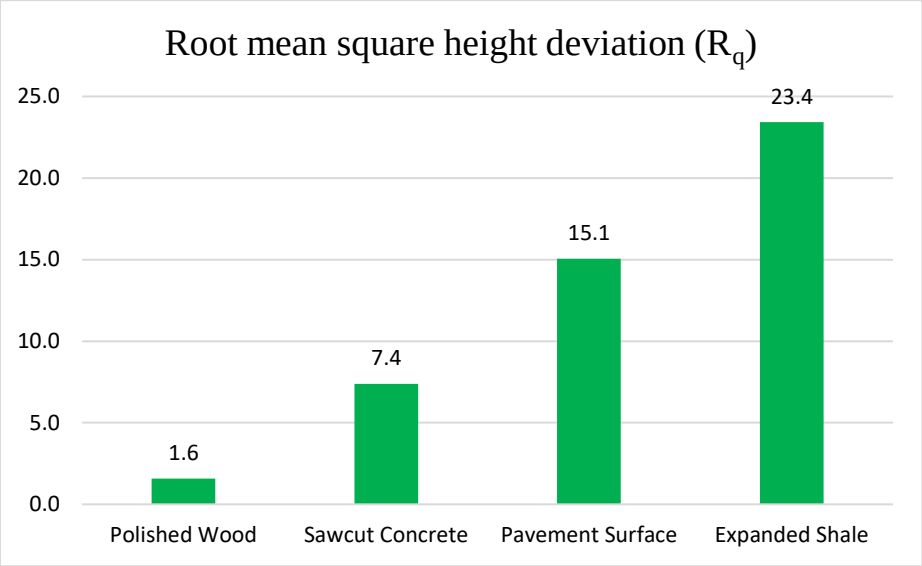

Figure 10 – R_q parameter for different surfaces

Surface area determination represents the texture of the surface and thus, as previously noted, the greater the surface projections or depressions, the higher the surface area as shown in Figure 11.

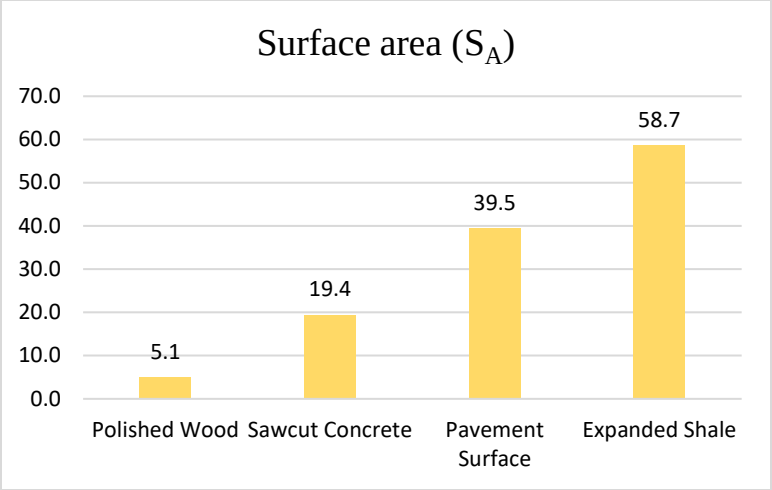

Figure 11 – S_A parameter for different surfaces

However, skewness and kurtosis did not show any significant trend for these surfaces. Out of all the surfaces, clean sawcut concrete had an abnormally high value of kurtosis of 4.24 as shown in Figure 12. This implies that surface deviations on sawcut concrete are highly irregular and lies on extreme ends of height distribution.

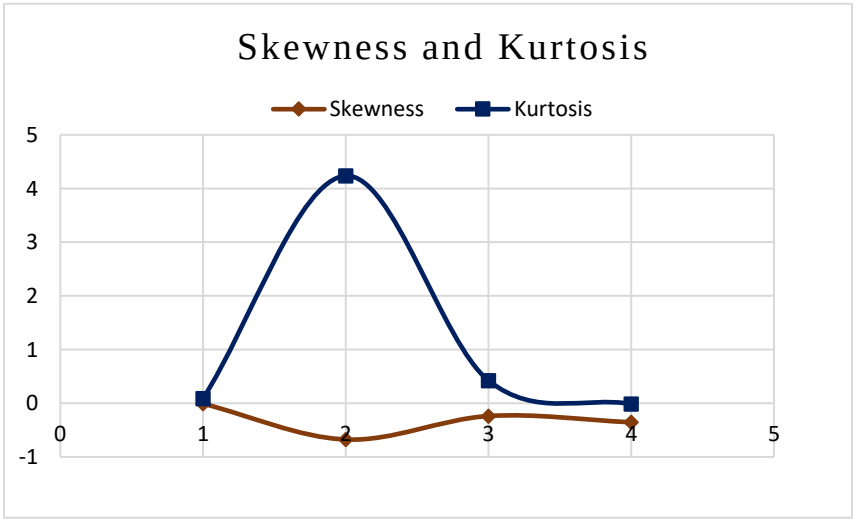

Figure 12 – Skewness and Kurtosis of different surfaces

This ability of Image J software to quantify surface characteristics was verified further in this research to differentiate between clean and dirty surfaces by establishing threshold values of these surface parameters**.**

IMAGE ANALYSIS - DETECTION OF DIRT

Concrete is an inherently rough material with peaks and depressions, and dirt particles from field slurry are small enough to fill these empty spaces upwards progressively. After a particular threshold value, these dirt particles act as a physical barrier between joint wall and sealant.

Surface Preparation

The concrete surfaces were treaded with a slurry of known solids concentration reconstituted from dehydrated saw cut slurry. Original concentration of field slurry was 34g of solids per 100ml of water. The solids were obtained from the dried saw slurry and then reconstituted to a concentration 20g/100ml of water. Successive dirt levels were achieved by increasing the concentration in steps of 20g/100ml of water. Surfaces were prepared with three different concentrations 20g/ml, 40g/ml and 60g/ml, of dirt solution, with one surface being wiped clean for any presence of dirt. These surfaces were dried with a heat gun, and image analysis was conducted after drying to produce four cleanliness states D0, D1, D2, and D3, with increasing order of dirtiness.

Verification with Imaging Data

These surface 3D plots show a significant change in texture when dirt is added to the rough concrete surface as shown in Figure 13.

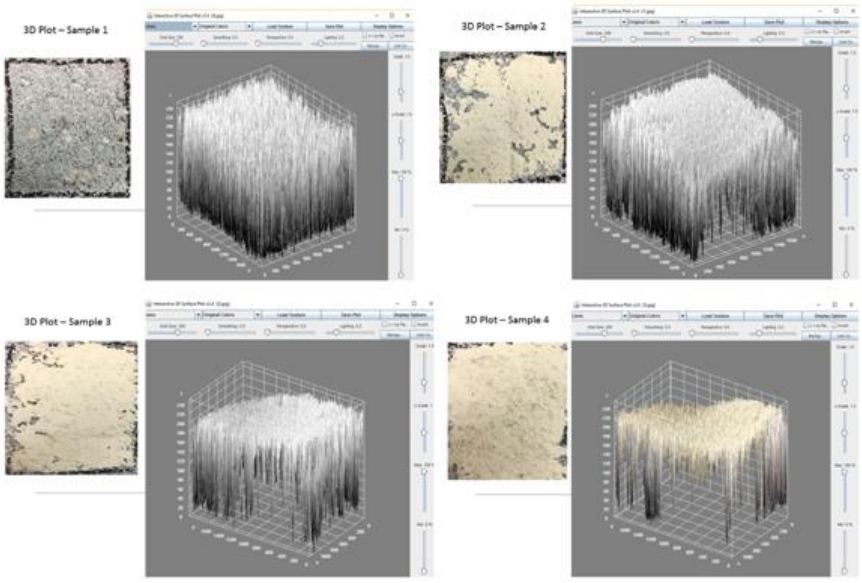

Figure 13 – Smoothening of surface plots with successive dirt

As evident from Figure 14 & Figure 15, surface height parameters like root mean square deviation height and total height show a considerable decrease with increase in dirtiness.

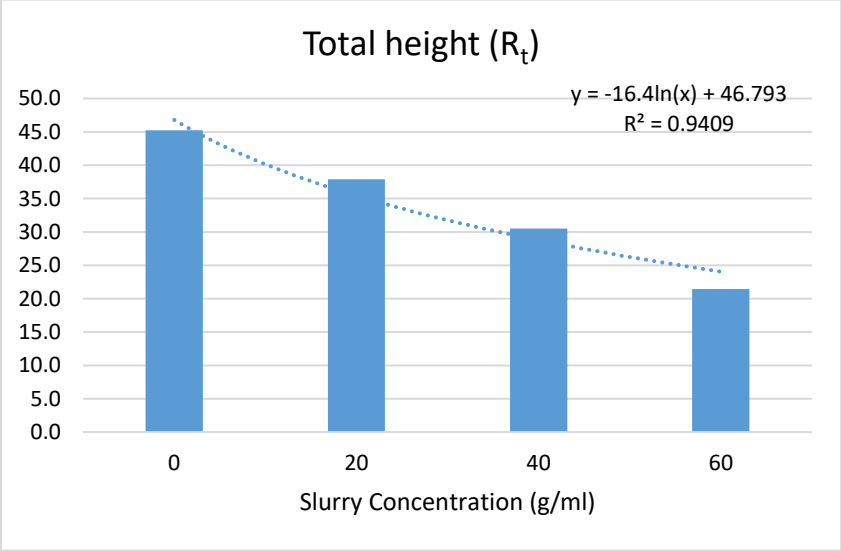

Figure 14– R_t parameters with increasing levels of dirtiness

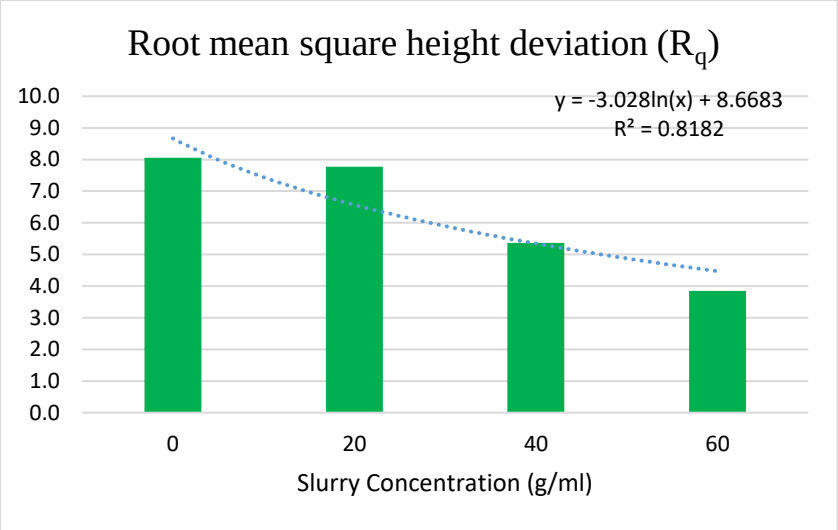

Figure 15– R_q parameters with increasing levels of dirtiness

These two parameters are calculated locally. Thus, parameters were able to capture changes in surface texture closely. All these parameters show a logarithmic relation with concentration of surface contamination. There is also a significant decrease in surface area along with the successive addition of dirt, confirming the smoothening of the rough surface due to dirt accumulation as shown in Figure 16.

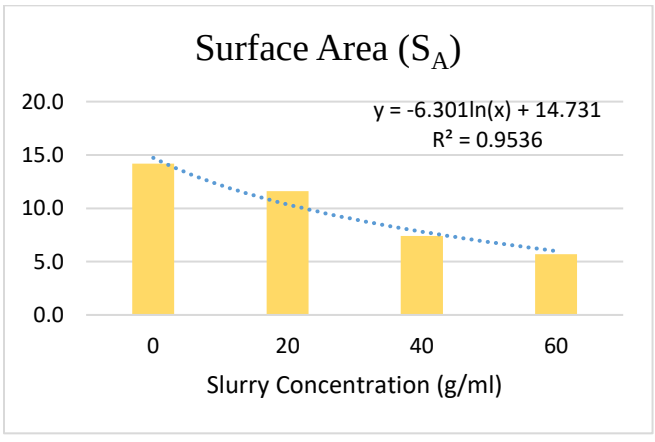

Figure 16 – Decrease in surface area with increasing levels of dirtiness

Skewness and kurtosis have the potential of being essential parameters as they are able to indicate the biased nature of surface height distributions. Preliminarily, there was a decrease in both skewness and kurtosis values upon increasing dirt levels. Thus a smoother texture with each addition of dirt level, as apparent in Figure 17. Abnormal values of skewness and kurtosis may reflect a significant surface irregularity.

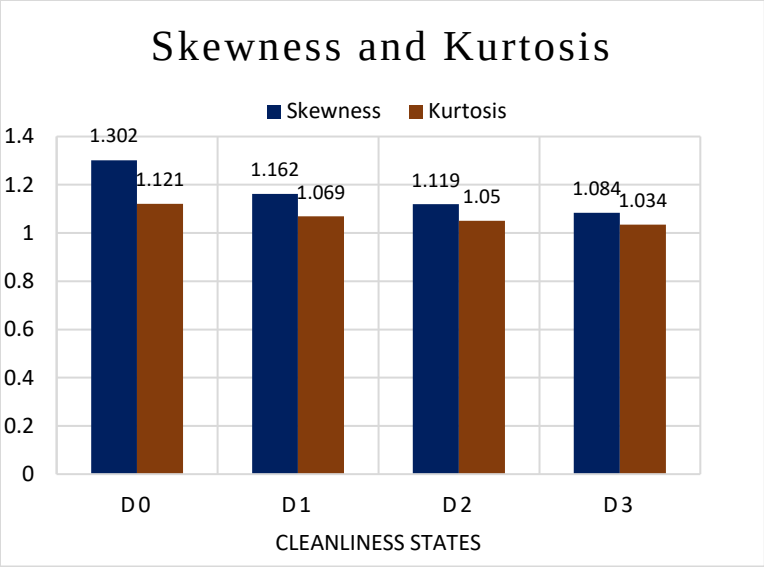

Figure 17 – Skewness and Kurtosis parameters vs. Cleanliness states

IMAGE ANALYSIS – STATISTICAL ANALYSIS

Two separate concrete samples were prepared to get imaging data on the surface roughness of sawcut concrete. After curing for 28 days, 1ft long rectangular blocks of concrete were sawcut in the middle to yield two joints each of dimensions ½ inch width and 1’ depth. Sawed surfaces were wiped with a clean lint-free dry cloth and applied with one coat of dirt slurry having 20g of solids

per 100ml of water. After drying for one day, images were acquired from each side of sawcut joints. Multiple images were captured along the length of the sample with the help of joint inspection device before and after slurry application and analyzed using Image J software.

Among multiple parameters generated, three parameters were chosen for statistical analysis. These were the root mean square deviation height (R_q), Total height (R_t) and Surface area (S_A). Rest of the parameters were unable to show any significant changes with dirt application. However, high values of Kurtosis (R_{ku}) greater than 3, were generally associated with clean concrete surfaces in both samples. There is a decrease in sharp features of concrete profile due to the addition of dirt particles. Figure 18 shows a decrease in R_t parameter of concrete surface upon application of dirt.

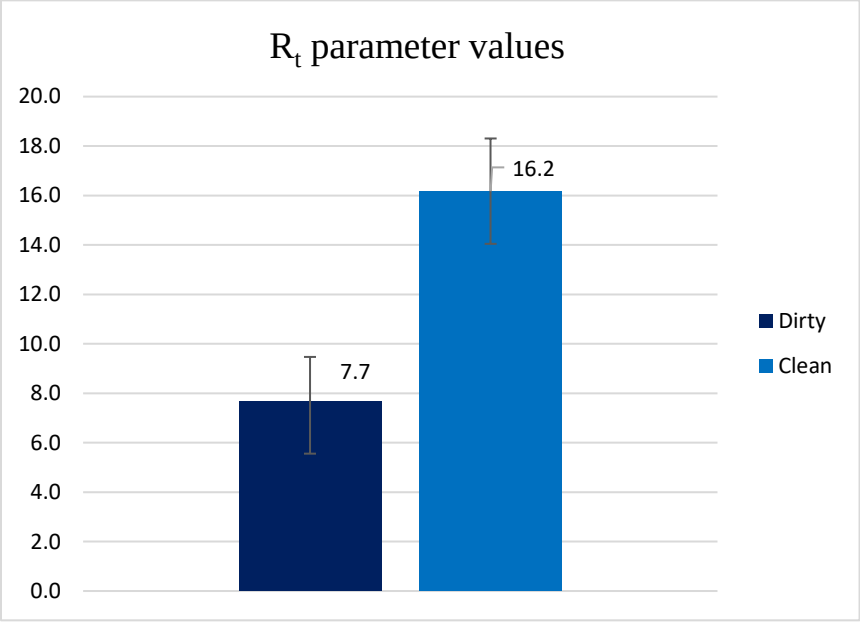

Figure 18 – R_t parameter values for clean and dirty states of concrete

Similar trends were observed for R_q and S_A parameters as shown in Figure 19 and Figure 20.

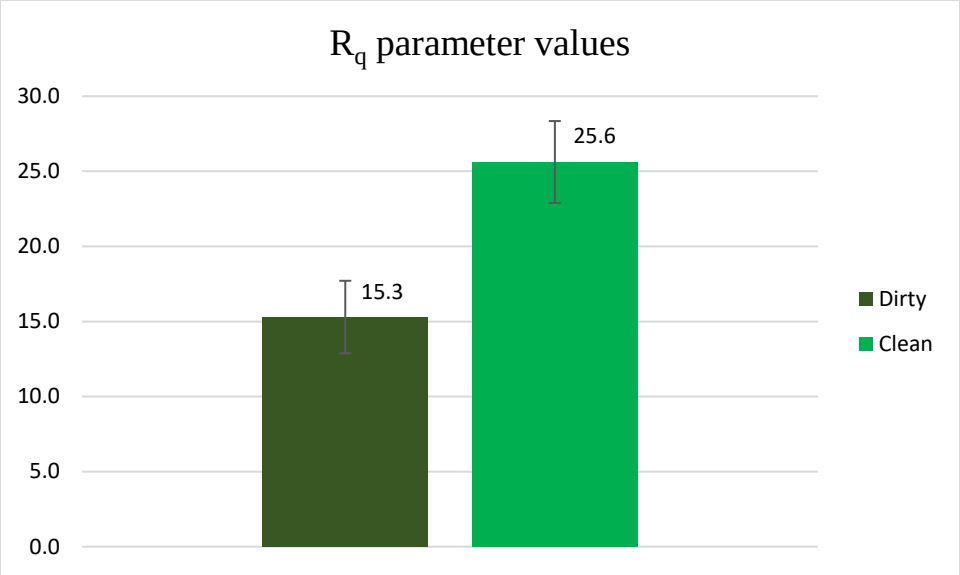

Figure 19 – R_q parameter values for clean and dirty states of concrete

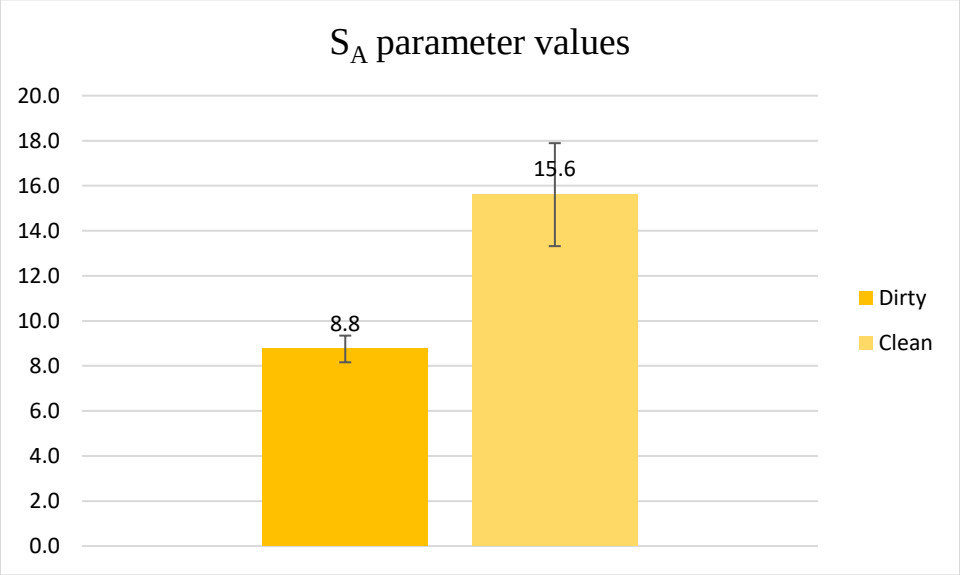

Figure 20 – S_A parameter values for clean and dirty states of concrete

These parameters were tested for the significant difference between clean and dirty states by hypothesis testing. Obtained p-values were almost negligible, negating the null hypothesis of no

significant difference between values of these parameters in clean and dirty states. Statistical analysis was done to find best-fit distribution for these three parameters. Figure 21 and Figure 22 show the probability plot for R_q parameter for clean and dirty states respectively.

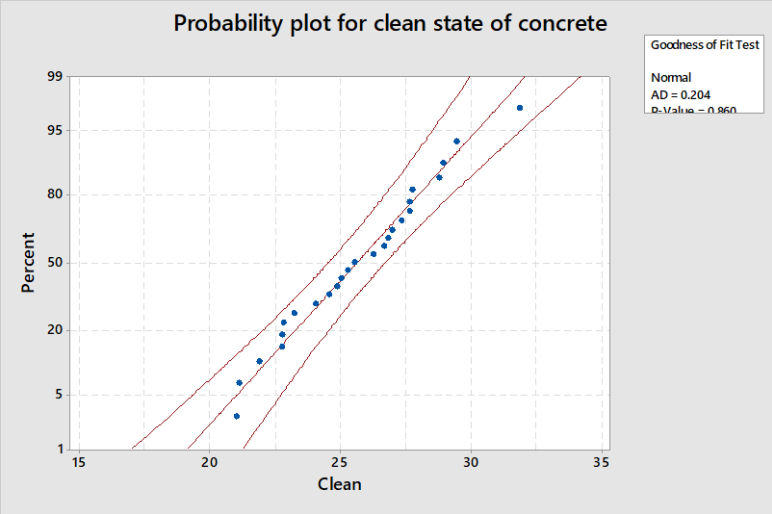

Figure 21 – R_q parameter goodness of fit for clean state of concrete

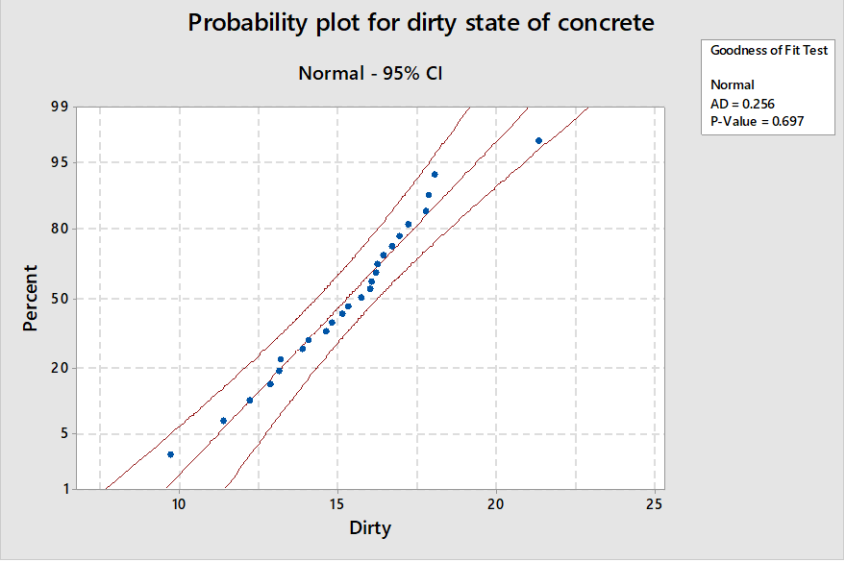

Figure 22 – R_q parameter goodness of fit for the dirty state of concrete

It was found that R_q parameter exhibit normal distribution with most of the data points within confidence bound. Other parameters didn't show such high level of goodness of fit. Based on these observations, normal distributions of R_q are used to describe clean and dirty states of concrete in next part of study.

A vital aspect of this characterization is the collection of sufficient data to determine the Type I and II errors with regard to surface area with respect to minimum acceptable cleanliness or maximum dirtiness levels. Type II error was calculated for R_q, which came out to be negligible at $\alpha = 0.05$. As shown in Figure 23, Type I and II errors distinguish the difference between clean and dirty areas of the joint face and hence can establish a basis for QC/QA for sawcut joint cleaning. Type I error is associated at producer's end, which is the probability of rejecting a good product by the consumer as a bad product. Type II error is risk associated at consumer's end that a defective product will pass the quality tests, which are devised to distinguish between defective and good product. The threshold illustrated in Figure 18 is established at a significant level of 5%.

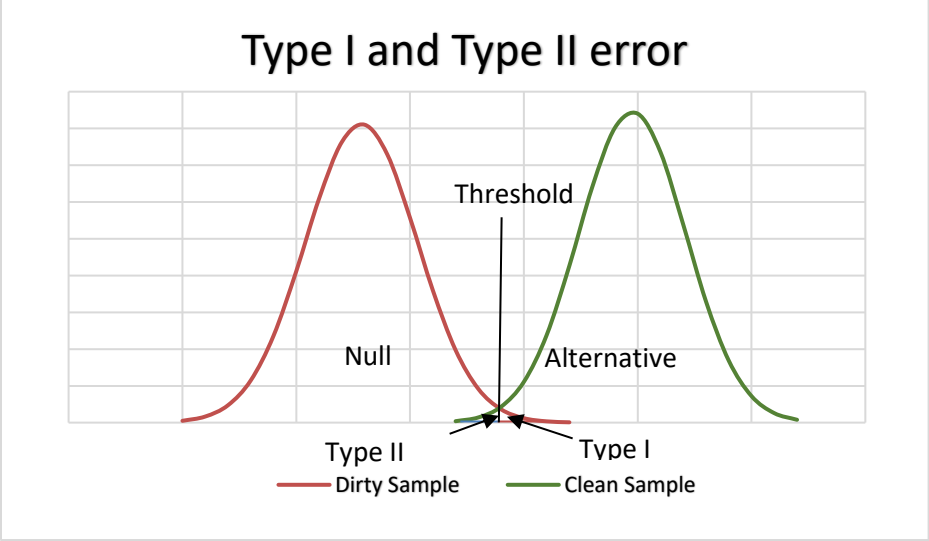

Figure 23 - Graphical representation of Type I and Type II error

Thus a Type II error indicates the quality of a process, which is this case Type II error provides a clear indication to the owner of the risk associated with installation as the basis for the specification for construction quality control**[33]**. Table 3 gives threshold value for parameters R_q for the clean state of concrete.

Table 3 – R_q parameter for the clean state of concrete

Root mean square deviation height	
Mean	25.6
Standard Deviation	2.7
Threshold Value	20.2

These threshold values need to be tied down with sealant concrete adhesion in laboratory and sealant performance in the field, for better applicability of this method for field inspection. The clean results for concrete should serve as a standard reference.

Due to a clear distinction between clean and dirty values for both samples, the Type II error is negligible. Image J software is able to distinguish between the clean and dirty surfaces with a very small Type II error. This provides strong evidence that image analysis can be a reliable method to distinguish between clean and dirty surfaces in the context of sawcut concrete joints.

APPLICATION TO FIELD INSPECTION - EXAMPLE

Images of joints from O'Hare International airport pavements were taken after joint preparation using joint inspection device and analyzed using Image J software as an example of the application of this methodology to the field. The joint inspection device is able to acquire good quality images for analysis as evident in Figure 24.

Figure 24 - Field Image from Joint Inspection Device

Imaging data from field image was compared with the data of clean and dirty states of the concrete sample in the laboratory. Three parameters were compared – total height; root means square deviation height and surface area. As shown in Figure 25, field data values lie on the clean side of total height data range.

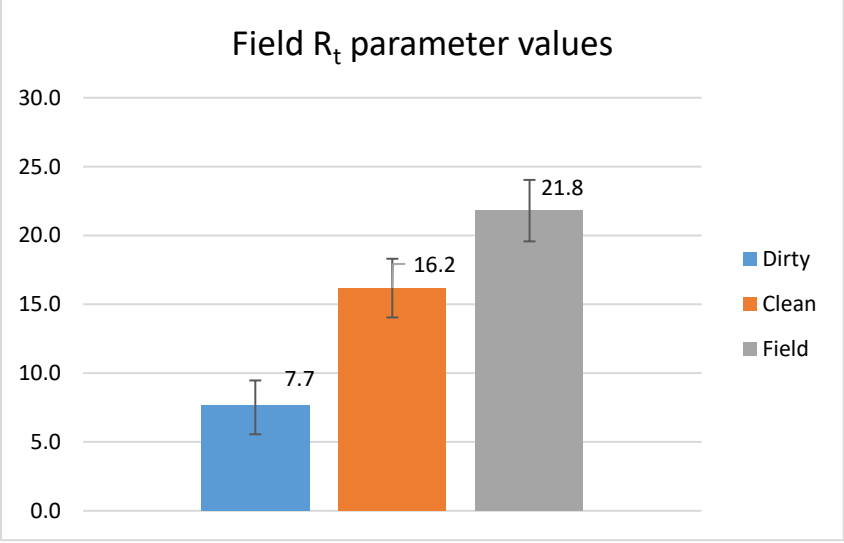

Figure 25 – Field data for total height parameter

However, for surface area parameter, field data values were between clean and dirty values from the laboratory as shown in Figure 26.

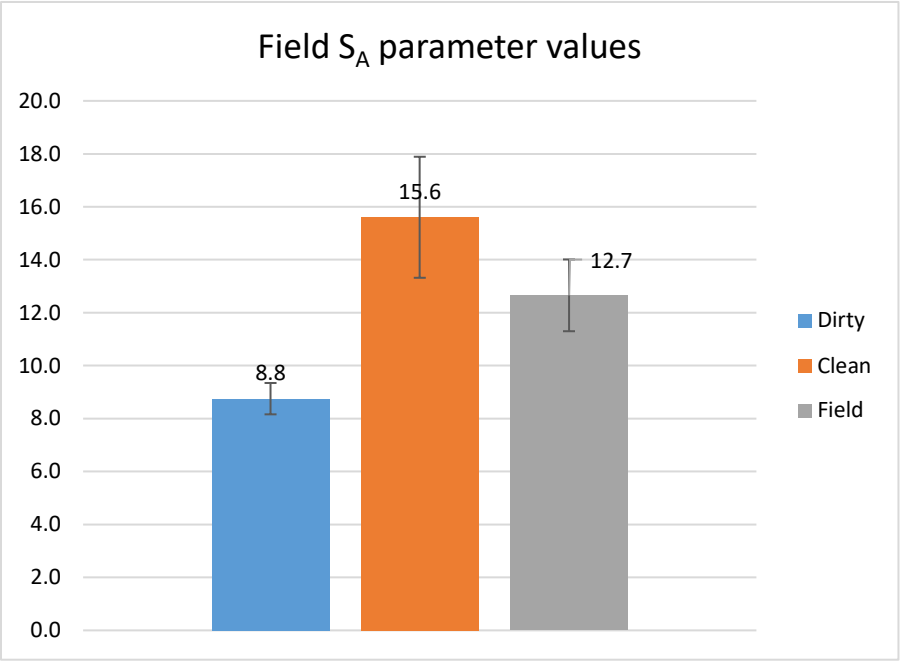

Figure 26- Field data for surface area parameter

As discussed earlier, R_q parameter exhibits normal distribution across both clean and dirty surfaces. Hence, this parameter was analyzed through comparison of normal distributions of field and laboratory data, as shown in Figure 27. These distributions imply a rougher surface without much dirt accumulation on the sawcut surface.

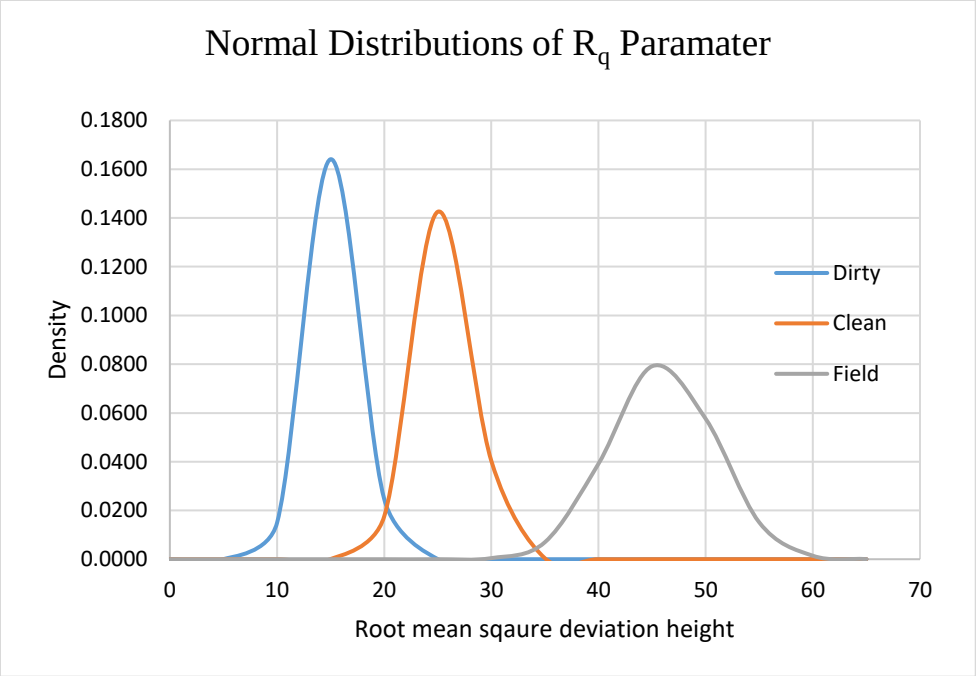

Figure 27 - Data spectrum for R_q parameter

As an aid to effective quality control, images gathered from joint inspection device should be immediately analyzed, and normal distributions of R_q parameter should be compared with reference clean and dirty states of particular concrete at the site. If the data lie on the dirty side of parameter spectrum, one more round of cleaning can be recommended. Otherwise, if the data lies on the clean side of the spectrum, sealant installation can be suggested. This normal distribution also show the need of calibration for specific methods of surface preparation including hydro blasting, sandblasting and air blasting, as these preparations produce difference roughness characteristics on the sawcut concrete surface. This may be the reason for such high value of R_q for field data.

This method needs parameter calibration with field data along with verification with associated long-term sealant performance of specific field conditions. Table 4 shows template for joint surface assessment using joint inspection device in the field.

Table 4 - Example of joint inspection device datasheet

Surface Assessment - Joint Inspection Device						
Parameter	R_q		**Units**			
Data Intervals	**Clean**	**Distribution**	**Dirty**	**Distribution2**	**Field**	**Distribution3**
0	15.1	0.0000	28.9	0.0000		
5	13.2	0.0000	22.7	0.0000		
10	13.1	0.0129	24.8	0.0000		
15	13.9	0.2033	27.3	0.0000		
20	16.2	0.0027	28.8	0.0132		
25	18.0	0.0000	29.4	0.1424		
30	14.8	0.0000	27.6	0.0447		
35	12.9	0.0000	25.3	0.0004		
40	17.8	0.0000	25.0	0.0000		
45	12.2	0.0000	25.5	0.0000		
50	11.3	0.0000	21.0	0.0000		
55	14.0	0.0000	27.6	0.0000		
60	15.3	0.0000	27.0	0.0000		
65	14.6	0.0000	21.1	0.0000		
Avg	14		26			
SD	2		3			

The imaging data can also be used to identify locations which fall below the threshold value of R_q parameter for the clean joint surface as shown in Figure 28, with red bars showing lowered surface area due to the presence of dirt. Further cleaning can be suggested on the basis of frequency and R_q values of the dirty joint locations. However, these data values and ranges are specific to the

joint inspection device and camera used in this study. These data sheets need device calibration before being applied to use as an aid for joint inspection in the field.

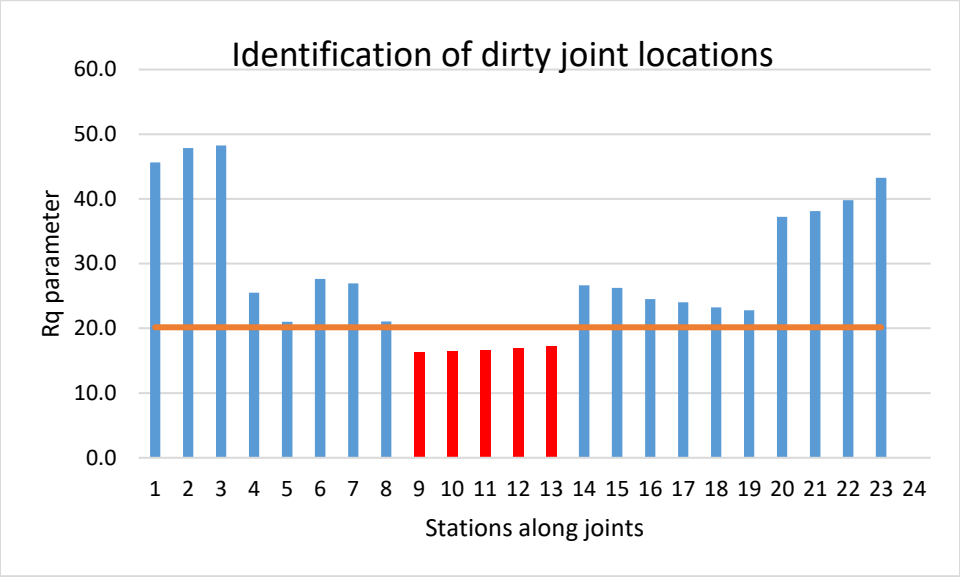

Figure 28 – Identification of dirty joint locations through imaging data

CHAPTER IV:

SEALANT-CONCRETE ADHESION – EXPERIMENTAL STUDY

The second part of research focuses on understanding the effect of dirt, moisture, and hydration on the development of the adhesive bond between sealant and concrete. Concrete specimens were sealed with silicone sealant at different levels of dirt and moisture contamination at different ages of concrete. Since sealants are supposed to cure fully in 21 days, development of adhesive bond within this time frame was studied only. Image analysis methodology and microwave technology were employed for indirect measurement of surface contamination by dirt and moisture, so that threshold values can be established.

INDIRECT MEASUREMENT OF MOISTURE

Earlier works like Lee and Zollinger (2012) have tried to establish a relationship between dielectric measurements and free water contents of fresh concrete with ongoing hydration process. Similar attempts were made in this laboratory study to develop a relationship between moisture contents and dielectric measurements for fully hydrated concrete [34].

Sample Preparation

Concrete samples were prepared with w/c ratio of 0.45 and air content of 4% using ACI mix design method. Fresh concrete was cast into beam molds of 4in*4in*12in and was allowed to cure for 3 months for full hydration. After curing, concrete beams were cut into rectangular blocks of size 0.5in*2in*3in with a hydraulic saw, to replicate smooth surfaces obtained in the field after saw cutting.

Moisture was assumed to be distributed uniformly over the concrete samples, and moisture levels were achieved by submerging samples in water until surface saturation and drying these samples in the oven for different time durations. Dielectric measurements were made using Percometer on the top surface of concrete specimen adjacent to surface to be sealed as shown in Figure 29. Percometer is a portable surface probe device, which measures the dielectric constant through a change in the electrical capacity of electrode probe in contact with the material.

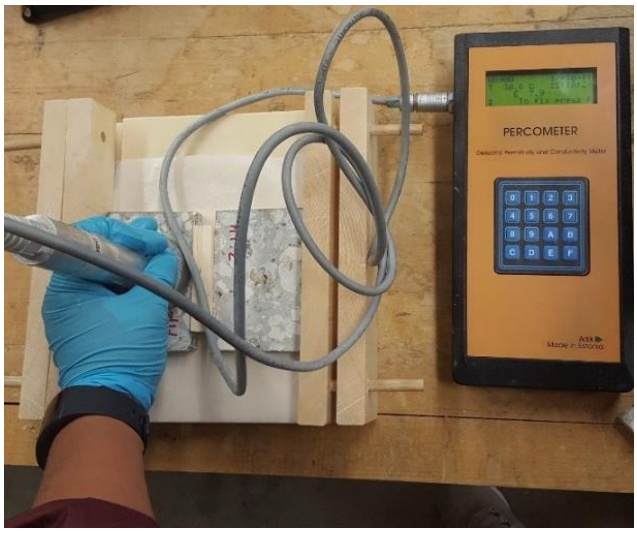

Figure 29- Dielectric measurement through Percometer

A calibration curve was developed correlating the measured dielectric values of concrete samples with free water contents of samples. Free water contents were calculated by dividing the weight of water with oven dried weight of the concrete specimen. The relationship between the dielectric constant and water content can be expressed by following formula:

MC % = 6.28*log DC -10.52

where DC is measured dielectric constant of the fully hydrated concrete sample, and MC % is free water content of the concrete sample.

It is essential to distinguish the degree of hydration of concrete, as dielectric constant values evolve with hydration process. Figure 30 shows the comparison between calibration curve obtained in this study and relationship established by Lee and Zollinger (2012) **[34]**. The significant difference between these observations is due to different timeframes in terms of degree of hydration. Lee and Zollinger's model is applicable to fresh concrete within 7 days of casting, while relationship developed in this study is for already hardened concrete with completed hydration.

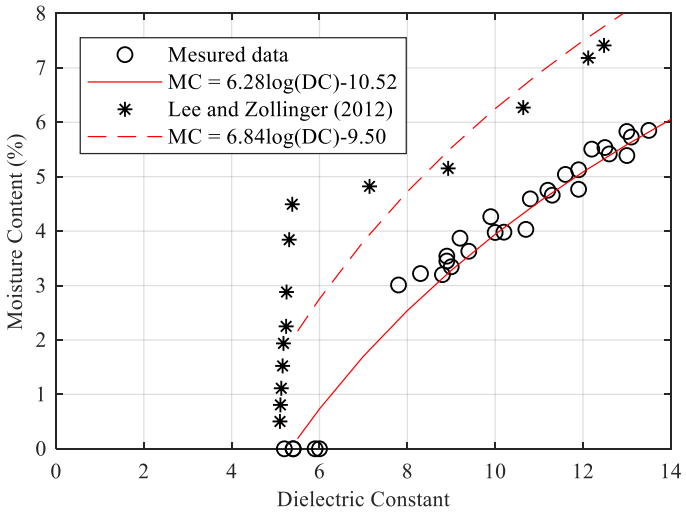

Figure 30 - Calibration models for dielectric constant and moisture content

The calibration curve based on dielectric constant measurements through percometer can be used as an effective indirect method to measure and monitor moisture states of concrete in the laboratory to evaluate sealant performance. Microwave technology is an efficient tool for indirect

measurement of volumetric water content, and isolated pockets of moisture can also be identified based on these measurements. For field application, a calibration curve based of microwave technology and developed for specific mix design of concrete at the site can be a useful tool in predicting moisture states in the field and further monitoring for better support to quality control operations. Most field inspection practice can identify only surface moisture; microwave technology has added advantage of being able to detect the free moisture inside concrete also. However, the particular shape and configuration of joint pose a problem in establishing points of contacts for accurate measurement.

EFFECT OF MOISTURE ON SEALANT CONCRETE ADHESION (FULLY HYDRATED CONCRETE)

The concrete specimens prepared for the moisture calibration study were bonded together in a pair with DOW 888, a silicone based sealant at different moisture states. Sealant beads of dimensions 0.5in*0.5in*3in were installed using caulking gun as shown in Fig 31.

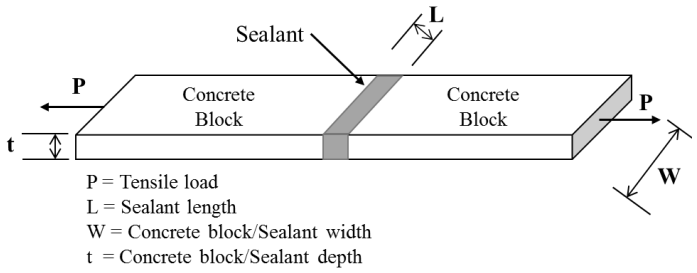

Figure 31 – Sealant-concrete specimen for tension test

Different moisture states were obtained with the help of air drying, and oven drying saturated concrete samples. Full saturation was achieved by soaking oven-dried samples in water for 2 days.

The moisture levels were closely monitored to achieve desired moisture contents with the help of frequent weight observations for the oven and air-dried samples. Moisture content measured in this study is free water content percentage with respect to oven dried weight of the concrete sample as reference.

Free water contents were calculated by using following formula:

MC % = Weight of water/weight of oven dried concrete sample

Three moisture states were obtained and categorized into following levels:

1.) Low Moisture Level (MC% = 1-2%)
2.) Medium Moisture Level (MC% = 3-4%)
3.) High Moisture Level (MC% = 5-6%)

For every moisture level, two specimens were prepared to result in total six samples. Specimens were wiped with a clean, dry and lint-free cloth before sealant application.

Image Analysis – Detection of Moisture

Imaging data were collected with an endoscopic camera without joint inspection device to suit the configuration of the tensile test specimen. Specimens were imaged on the surface to be sealed at different moisture states just before the sealant installation. Skewness and kurtosis values were abnormally high for the dry and clean surface at 0% moisture content as shown in Figure 32.

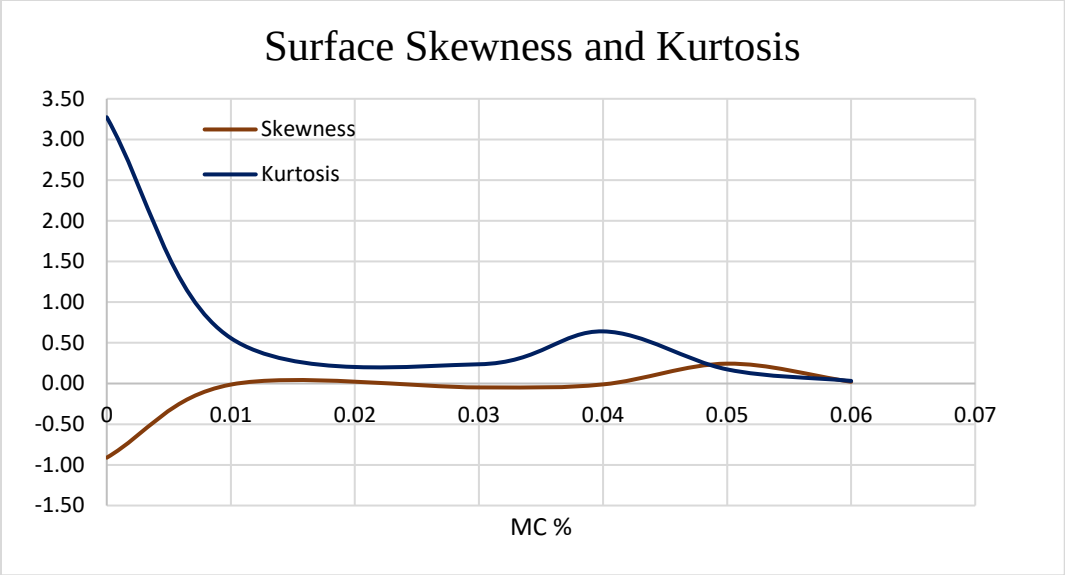

Figure 32 - Surface texture variation with increasing MC%

Unlike dirt, Image J parameters showed little sensitivity to moisture levels at concrete surface, as moisture is uniformly distributed over the volume rather than on the surface only. Image J parameters are sensitive to surface properties, thus will be more reflective of changes in surface moisture. Therefore, it won't be able to give a comprehensive picture of free moisture beneath the concrete surface. Microwave technology can detect free moisture in concrete microstructure also, thus will be more appropriate for moisture detection and monitoring in case of rigid pavement joints.

Verification with Tensile Bond Testing

Bonded specimens were allowed to be a cure for 28 days at room temperature before tensile bond testing. Tensile deformation was applied by an Instron tensile meter (Model 5943) at the rate of 500mm/min until failure. All specimens exhibited adhesive failure, an, i.e., detachment of silicone

sealant from the concrete surface. True stresses and strains were calculated using following formula:

$$\sigma_t = \sigma_e (1 + \varepsilon_e)$$

$$\varepsilon_t = \ln(\frac{L_i}{L})$$

Where σ_t and ε_t are true stress and strain respectively, ε_e is engineering strain calculated from the instantaneous length (L_i) and initial length (L).

Stress-strain behavior was observed for specimens at three different moisture levels. Stress-strain patterns before debonding were similar for all moisture levels as shown in Figure 33. The nominal ultimate true stress to failure was within the range of 0.38 -1.83 MPa (55-265 psi). Average tensile bond strengths were higher at lower moisture levels.

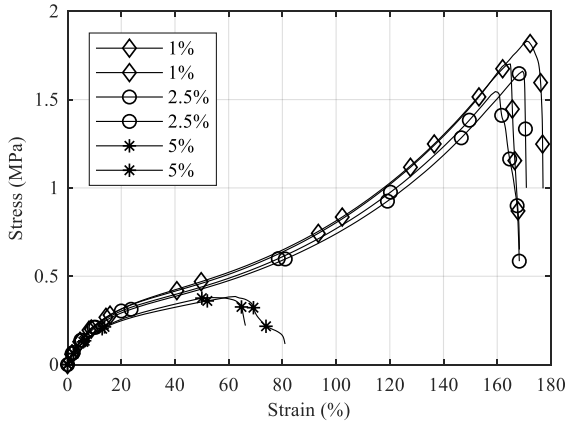

Figure 33 - Stress-strain curves at different moisture levels

A tensile bond strength model was developed to establish a relationship between moisture content and ultimate strength, given by following formula:

$\sigma_b = 1.64\text{-}0.095(MC\%)^2 + 0.22MC\%$

where σ_b is true stress to failure in MPa, and MC% is free water content as a percentage by weight.

Tensile bond strengths are an indirect measurement of adhesive bond developed in initial stages of sealant installation. The sealant is assumed to be fully cured within 21 days; thus after that, there is little bond formation between the sealant and concrete [35]. The average tensile bond strengths with increasing moisture contents are given in Figure 34.

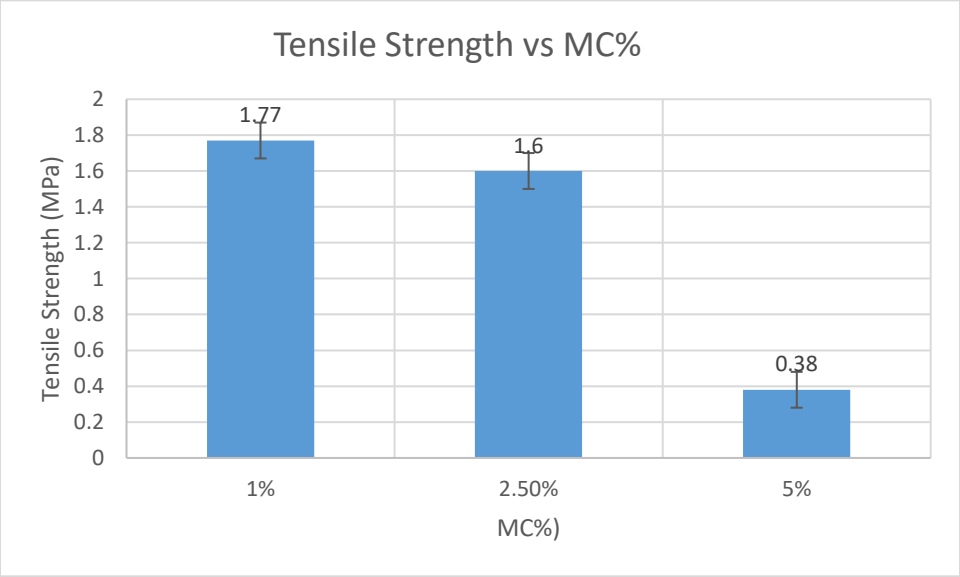

Figure 34 - Ultimate tensile bond strength vs. Moisture content

The experimental study showed that bond strengths have high sensitivity at higher moisture levels. Sealant performance can be predicted if a proper correlation between bond strengths, MC%, and DC can be established. The results indicate a threshold value for free water content below which

moisture has no effect on sealant concrete adhesion. Since these tests deal with volumetric water content rather than surface moisture, the importance of monitoring the volumetric water content in the field is recognized as bond strengths observed were sensitive to free water content.

Relationship between Indirect Measurement of Moisture and Tensile Bond Strength

Both image analysis and dielectric measurements were employed in this study to indirectly measure the moisture content of concrete samples. However, the DC measurements with percometer were more accurate in capturing the changes in free moisture content. This accuracy of microwave technology in predicting moisture content can prove to be a useful technology in predicting moisture state of joint for quality control at the time of sealant installation.

EFFECT OF MOISTURE AND DIRT ON SEALANT CONCRETE ADHESION (INITIAL SEALING CASE)

This second study on sealant concrete adhesion focuses on sealing of still hydrating fresh concrete. As discussed, earlier porosity and capillary tension are different in case of sealing fresh concrete and sealing fully hydrated concrete. Therefore, these two needed to be studied separately.

To simulate the sealing of fresh concrete sawn surfaces, the tensile bond test specimens were prepared for fresh concrete samples at the age of 7 days. Concrete samples were prepared with w/c ratio of 0.45 and sawcut with a hydraulic saw at the age of 7 days, into rectangular blocks of size 0.5in*0.5in*4in.

Three moisture states – M1, M2, and M3 were achieved through following methods:

M1-5 minutes of heat gun after air drying for an hour

M2-Air drying for an hour

M3-Surface saturation with water

These moisture states were combined with three dirt states namely D1, D2, and D3. These were achieved by applying fixed weights of dried field slurry in following proportions:

D1-No artificial dirt application, only dirt present is from the sawcutting procedure

D2-Application of 1g of dried slurry solids on the surface to be sealed

D3-Application of 3g of dried slurry solids on the surface to be sealed

Total 27 samples were prepared for each of the 9 combinations namely M1D1, M1D2, M1D3, M2D1, M2D2, M2D3, M3D1, M3D2, and M3D3 as shown in Table 5.

Table 5 – Dirt and Moisture combinations for surface preparation

	Dirt Levels		
Moisture Levels	M1D1	M2D1	M3D1
	M1D2	M2D2	M3D2
	M1D3	M2D3	M3D3

Concrete blocks were sealed as soon as the desired surface state was achieved. A caulking gun was used to seal samples with silicone based DOW 888 sealant with sealant beads of size 0.5in*0.5in*3in. Samples were cured for 28 days at room temperature to ensure full development of the adhesive bond between concrete and sealant.

Image Analysis – Detection of Moistures and Dirt

Images were captured for each surface state using the endoscopic camera without joint inspection device to suit the configurational constraints of joints and processed using Image J software to get surface height and surface area parameters. All parameters of interest R_t, R_q, and S_A, showed a significant decrease with increasing dirt levels at each moisture level. Figure 35 shows decreasing root mean square deviation height (R_q) with increasing dirt at all three moisture levels.

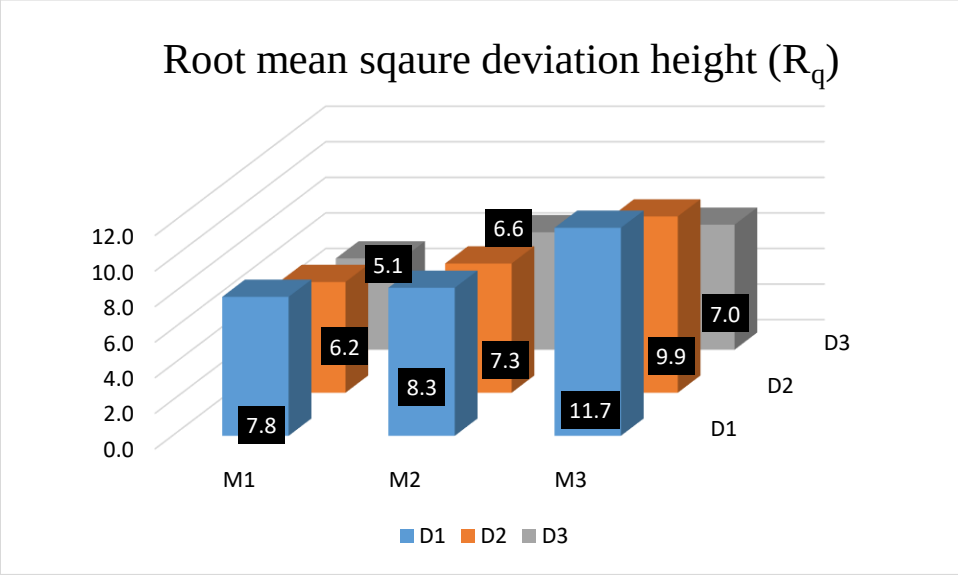

Figure 35 – R_q parameter at different surface states

Image J software can easily detect changes in surface texture due to the addition of dirt. However, it is difficult to distinguish between different moisture levels based on imaging data, as there is no significant trend.

Verification with Tensile Bond Testing

Tensile bond strength is a reliable parameter to reflect the quality of the adhesive bond between sealant and concrete at joint surface. Since this is a case involving fresh concrete sealed at the age of 7 days, the tensile bond strengths observed here were lower than the strength observed in the earlier study. Tensile bond strengths, in this case, were in the range of 0.39 MPa to 0.65 MPa. These were calculated by using following formulas:

$$\sigma_t = \sigma_e (1 + \varepsilon_e)$$

$$\varepsilon_t = \ln(\frac{L_i}{L})$$

Where σ_t and ε_t are true stress and strain respectively, and ε_e is engineering strain calculated from the instantaneous length (L_i) and initial length (L).

Figure 36 and 37 shows the true stress-strain curves for various dirt levels for M1 and M2 moisture states respectively.

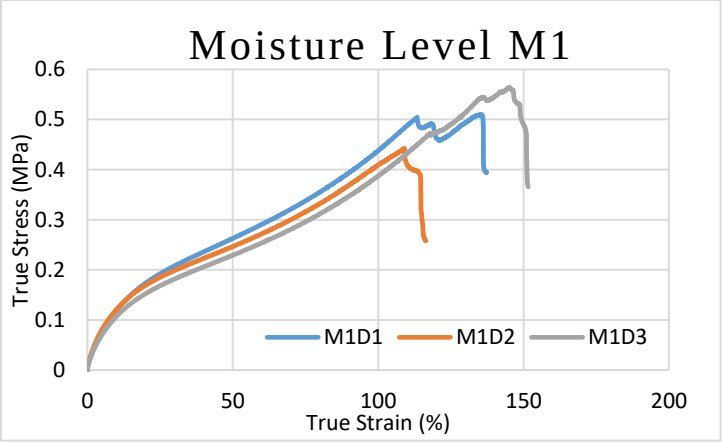

Figure 36 - True Stress-strain curves at Moisture Level M1

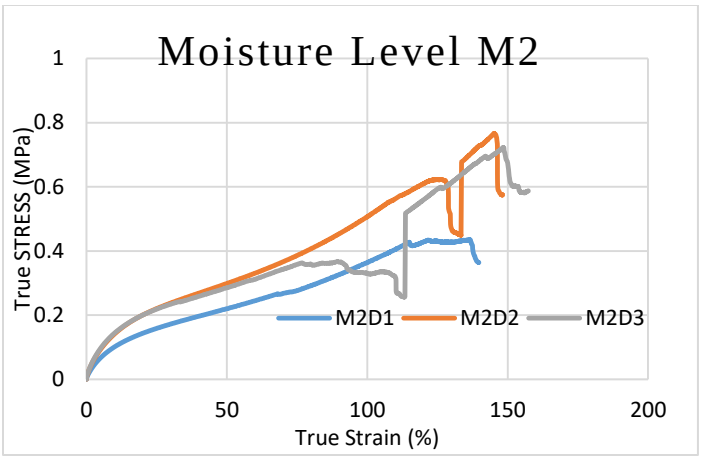

Figure 37 - True Stress-strain curves at Moisture Level M2

Stress-strain patterns were similar for all cases. The effect on tensile bond strength was maximum for specimens sealed at M3 moisture state as shown in Figure 38. The failure occurred before 100% strain for specimen sealed at M3D3 state.

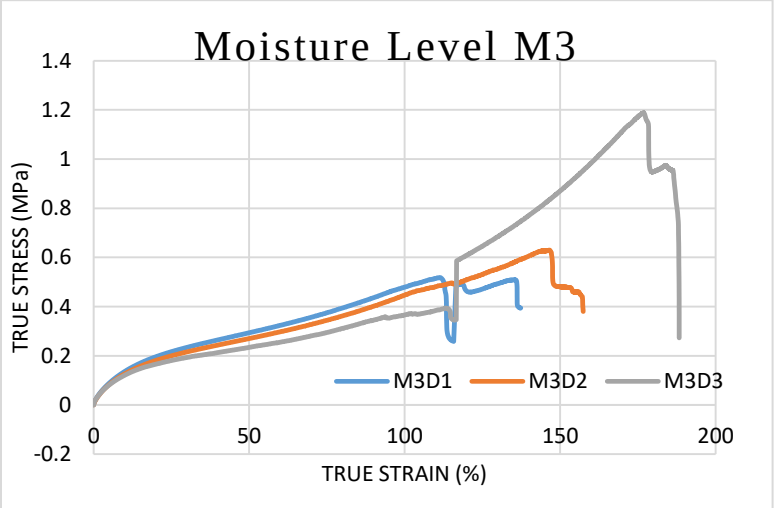

Figure 38 -True Stress-strain curves at Moisture Level M3

There was a general trend of decrease in average tensile bond strengths with increasing amount of surface contamination with dirt and moisture as shown in Figure 39. Tensile bond strengths were measured at failure state marked by either adhesive or cohesive failure. There was no case of cohesive failure showing that sealant has cured sufficiently gaining adequate strength. However, there were a couple of cases where aggregates were pulled out of concrete with sealant upon testing. Results from these cases were discarded. Samples having high states of moisture and dirt showed failures earlier than samples with less of these contaminants on the sample surfaces.

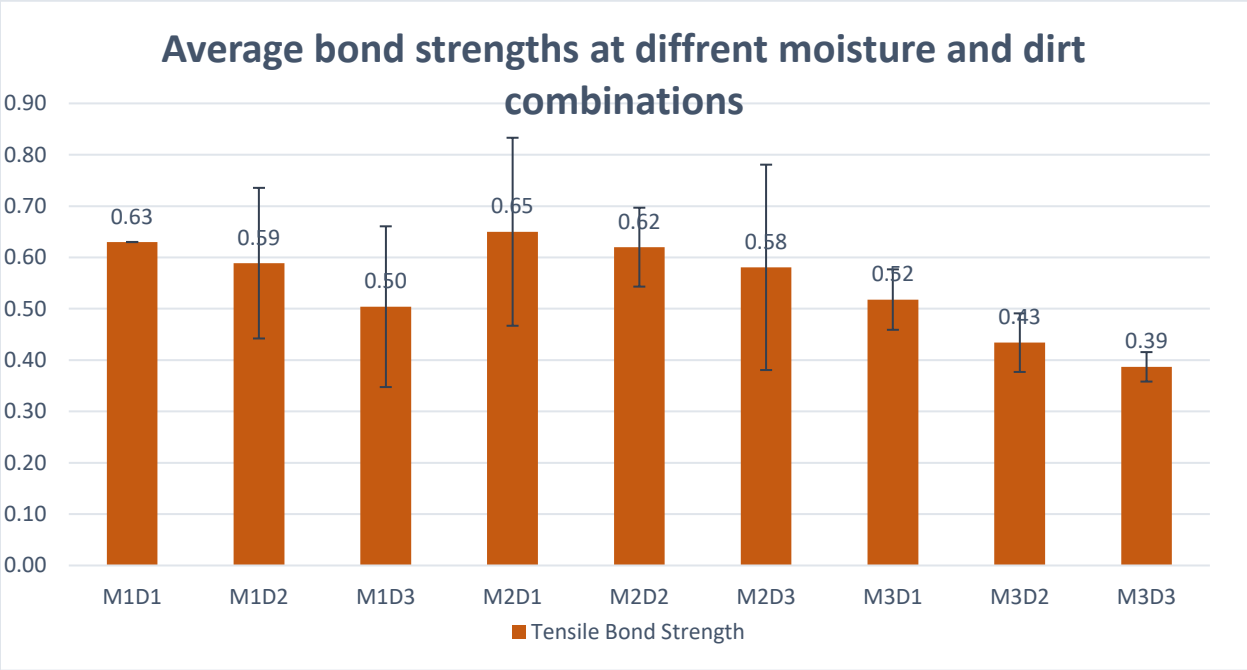

Figure 39 -Tensile bond strengths at different surface states

M1 and M2 moisture levels are more closely related to field conditions, as compared to M3, which is a surface saturated moisture state. M3 moisture level is very high and ordinarily visible water is

left out to dry before sealant application. M3 moisture level will mostly be encountered in small pockets at joint surfaces with not enough drying time. Effect of dirt gets highly pronounced when a high amount of moisture is present, as evident by lowest values of tensile bond strength at M3D3 surface state.

However, there are high values of tensile strength at surface states with intermediate states of both moisture and dirt, especially at M2 states. This implies for stronger adhesion when both dirt and moisture are present at moderate amounts on the interface. WJE studies have also reported abnormal bond strength when both dirt and moisture are present at the sealant concrete interface. Factorial design analysis was done to check if there is any strong interaction between moisture and dirt parameters. However, the individual effects of moisture and dirt came out to be more pronounced in affecting the sealant concrete bond strength. Tensile bond strength was observed to be more sensitive to the moisture than dirt. Pareto analysis of same is shown in figure 40.

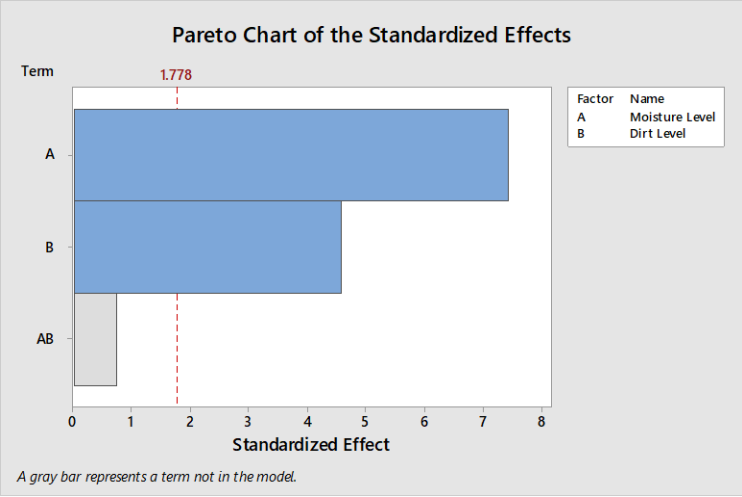

Figure 40 – Effects of moisture and dirt on bond strength

Thus, threshold criteria for the combination of these moisture and dirt states should be considerably higher than the levels analyzed in this study. Thus, further testing is needed to establish threshold values for these contaminants. This may be due to high capillary suction in concrete, ultimately pulling dirt and moisture solution into concrete microstructure itself. This is a case possible only when sealing fresh concrete.

Since M3 and D3 surface states are the ones that are really affecting the bond strength, a relationship was developed between root mean square height deviation parameter and tensile strength for these levels of moisture and dirt given by following formula:

$\sigma_b = 15.51\ln(R_q) + 22.17$

where σ_b is tensile bond strength in MPa and R_q is root mean square height deviation parameter in normalized units.

This equation is valid only for the specific instrument and camera used in this study. For application to other studies, device calibration is suggested.

There is a need for establishing threshold criteria for moisture and dirt quantity on joint surface, below which there is no significant effect on sealant concrete adhesion. Due to different stages of hydration involved in sealing fresh concrete and sealing old concrete, these threshold criteria should be different. It is practically impossible to get a direct measurement of quantities of these surface contaminants in the field. Therefore an indirect measurement methodology is necessary to ensure adequate quality control in the field for optimum adhesion.

CHAPTER V

CONCLUSIONS AND RECOMMENDATIONS

This study was aimed at understanding the adhesion aspect of joint sealant performance and how surface contaminants like dirt and moisture can be monitored in the field at the time of sealant installation for optimum adhesion between sealant and concrete. The following conclusions were made from this study:

1.) The surface assessment of saw cut joints on different types of concrete confirms the reduction in roughness of surface upon introduction of dirt. Image J software can capture the roughness changes in concrete surfaces and is also able to distinguish between smooth and rough surfaces with the help of surface height and area parameters.

2.) The main parameters studied in this research were total height (R_t), root means square height deviation (R_q), skewness (R_{sk}), kurtosis (R_{ku}), and surface area (S_A). However, root means square height deviation (R_q) parameter can be preferred to quantify surface texture as it is observed to be normally distributed over the concrete surface. Skewness and kurtosis parameters didn't show much sensitivity to changes in surface texture. However, very high values of kurtosis were generally associated with clean and dry sawn concrete surfaces.

3.) High roughness parameters imply less dirt on the surface and increased surface area for the sealant to bond with the concrete. The roughness parameters based on the clean surface values could serve as a standard for field inspection with joint inspection device along with quantifying the owner's risk at the time of sealant application.

4.) Image J is recommended for surface assessment only for dirt particles in the field and laboratory, while moisture detection is possible through the use of microwave technology like Percometer in the laboratory. A combination of these technologies can be used to characterize surface states of joint surfaces.

5.) There exist threshold values of dirt and moisture on the joint surface, below which these contaminants do not have any significant effect on quality of adhesion between sealant and concrete. Levels analyzed in this study seemed to be within the threshold values, as they were unable to produce any significant effect on sealant-concrete adhesion.

6.) The fresh sealing and resealing conditions should be studied and analyzed separately for detection of surface contaminants. The threshold for surface contaminants for optimum adhesion between sealant and concrete are different for both cases.

The strength of this research lies in its potential of field application of joints. The following recommendations were made, which could enhance this methodology for better field application:

1.) Further bond testing is needed to establish threshold values of contamination which are significantly detrimental to sealant-concrete adhesion.

2.) Joint inspection device can be optimized by additional microwave based moisture sensing technology, for a comprehensive field inspection in terms of moisture and dirt on the joint surface.

3.) Field calibration of the joint inspection device should be done for various sites, and surface assessments should be correlated with the long-term performance of sealant in the field.

4.) Clean and dirty states should be explicitly defined for sawn surface cleaned by particular cleaning techniques including waterblasting, airblasting and sandblasting. Different methods of cleaning produce different textures and Image J software can create a useful database for specific cleaning methods employed in the field.

5.) Quality of image analysis should be updated regularly with new imaging techniques available.

REFERENCES

1. *"*Concrete Pavement Joints"; *Technical Advisory T 5040.30 Concrete Pavement Joints*,FHWA,1990

2. "Guidelines for Routine Maintenance of Concrete Pavements." *Texas Transportation Institute*, 2008, No. P 0-5821, College Station, Texas.

3. "Standard Specification for Cold Applied, Single Component, Chemically Curing Silicone Joint Sealant for Portland Cement Concrete Pavements." ASTM 5893, West Conshohocken, PA.,2016

4. Ray, G. K. "Pavement Joint Sealing – Where Are We and How Did We Get Here?" *ACI Special Publication*,1986, 94-21, pp.371 – 377.

5. Morian, D.A. and S. Stoffels, "Joint seal practices in the United States: Observations and considerations." *Transportation Research Record: Journal of the Transportation Research Board*, 1998. 1627(-1): p. 7-12.

6. Peterson, D. E. "Resealing joints, and cracks in rigid and flexible pavements." *Synthesis Rep. 98. Nat. Cooperative Hwy. Res. Program, Transp. Res. Board. Washington*, D.C. 1982

7. Biel, D.T, and Lee, H., Performance study of portland cement concrete pavement joint sealants, *Journal of transportation engineering*, 1997, 23(5), 398-404

8. Hawkins, B.K., Ioannides, A.M. and Minkarah, I.A, *"*To Seal or Not to Seal? - A Field Experiment to Resolve an Age-Old Dilemma." *Transportation Research Record* 1749, 2014.

9. Shisler, III, F. W. and Klosowski, J. M. (1990), "Sealant Stresses in Tension and Shear," *Building Sealants: Materials Properties and Performance, STP 1069, ASTM, Thomas F. O'Connor, Ed., Philadelphia, PA,* pp. 95-10

10. Federal Highway Administration (FHWA). (2006d). "High Performance Concrete Pavements." Chapter 27. Ohio 1, 2, and 3 (US Route 50, Athens).

11. Gurjar, A., Zollinger, D. G., and Tang, T. (1996), "Laboratory Study of Strain and Age Effects on a Concrete Pavement Joint Sealant." *Presented at the 75th Annual Meeting of the Transportation Research Board, Washington, DC*.

12. ASTM. (2014). "Standard test method for adhesion and cohesion of elastomeric joint sealants under cyclic movement (Hockman cycle)."*ASTM C719, West Conshohocken, PA*

13. Khuri, M. F. “Analysis and Design of Incompressible Rubber Seals Using Experimental and Finite Element Methods.” *Ph.D. thesis, University of Michigan, Ann Arbor, Michigan*,1989

14. ASTM. (2018) “Standard Test Method for Adhesion-in-Peel of Elastomeric Joint Sealants.” *ASTM C794, West Conshohocken, PA.*

15. ASTM. (2013). “Standard Practice for Evaluating Adhesion of Installed Weatherproofing Sealant Joints” *ASTM D1521, West Conshohocken, PA.*

16. ASTM. (2012). “Standard test method for Indicating Moisture in Concrete by the Plastic Sheet Method” *ASTM D4263, West Conshohocken, PA.*

17. ASTM. (2017). “Standard Test Method for Measuring Moisture Vapor Emission Rate of Concrete Subfloor Using Anhydrous Calcium Chloride ”*ASTM F1869, West Conshohocken, PA*

18. FHWA(1999). *“*Materials and Procedures for Repair of Joint Seals in Portland Cement Concrete Pavements.” *FHWA Report No. FHWA-RD-99-146*

19. “Research of Test Methods Preparation for Sealing.” *West Coxsackie, THE SEAL/NO SEAL GROUP, NY Final* Report July 1, 2013, WJE No. 2011.0050

20. Li, Q., Crowley, R., Bloomquist, D. B., and Roque, R. “The Adhesive Strength Test (AST): A Newly Developed Test for Measuring Adhesive Strength of Sealant between Joints of Concrete Pavement.” *Journal of Materials in Civil Engineering, 2014’ Volume: 26.*

21. Anal K. Mukhopadhyay, Dan Ye, and Zollinger, Dan G., “Moisture-Related Cracking Effects On Hydrating Concrete Pavement,” Report to the Federal Highway Administration, Texas A&M Transportation Institute, The Texas A&M University System College Station, Tx, March 2014.

22. Powers, T.C., “Chemistry of Cement.” Proceedings of the Fourth International Symposium. Washington 1960 (National Bureau of standards [now National Institute of Standards and Techonology] Monograph 43), Vol. 2, pp. 577, 1962.

23. Pedro M.D. Santos and Eduardo N.B.S. Júlio. “A state-of-the-art review on roughness quantification methods for concrete surfaces.” *Construction and Building Materials ,2013,* Vol. 38,pp.912–923

24. Ammouche,A.,Riss,J.,Breysse,D.and Marchand,J. “Image analysis for the automated study of microcracks in concrete.” Cement and Concrete Composites,2001,Vol.23,pp267-278

25. Qi, C.,Weiss,J. and Olek,J.,"Characterization of plastic shrinkage cracking in fiber reinforced concrete using image analysis and a modified Weibull function." *Materials and Structures*,2003,Vol.36,pp 386-395

26. Akand, L., Yang, M. and Gao, Z., "Characterization of pervious concrete through image based micromechanical modeling." *Construction and Building Materials*, 2016,Vol.114, pp 547-555

27. In house Software Development, EMPA Material Science and Technology, https://www.empa.ch/documents/55996/86304/3D, Accessed Aug 2016

28. Characterization of cracks in cement-based materials by microscopy and image analysis, EMPA Material Science and Technology, http://www.calcolodistr.altervista.org/en/work/CrackSegment_TopDayImAnalII_MGriffa_2.pdf, Accessed Aug 2016

29. Klovas, A, and Daukšys, M. "The Evaluation Methods of Decorative Concrete Horizontal Surfaces Quality." *Materials Science*. Vol.19, No.3, July 229]013, pp.343-348

30. Chinga, G., Johnsen, P. O., Dougherty, R., Berli, E. L. and Walter, J., "Quantification of the 3D microstructure of SC surfaces." *Journal of Microscopy*, 2007 Vol.227, pp. 254–265.

31. *ImageJ User's Guide: IJ 1.46r*.ImageJ, 2012, pp. 139-143.

32. SurfCharJ – GCSCA. http://www.gcsca.net/IJ/SurfCharJ.html, Accessed Aug 2016

33. Alfredo,H.S., and Wilson,H.T. "Probablity Concepts in Engineering Planning and Design." JohnWiley & Sons, Inc., NewYork, 1998.

34. Lee, S. I., and Zollinger, D., 2012. " Estimating Volume Fraction of Free Water in Hardening Concrete by Interpretation of Dielectric Constant." JOURNAL OF MATERIALS IN CIVIL ENGINEERING, 24(2): 159-167

35. Dow Corning 888 Silicone Joint Sealant -Product Information Silicone Sealants

APPENDIX A

CONCRETE MIX DESIGN

Table 6 - Concrete Mix Design

W/C	0.45
Cement	565 lb/yd^3
Water	254 lb/yd^3
Air	4%
Coarse aggregate	1994 lb/yd^3
Fine aggregate	1197 lb/yd^3

APPENDIX B

TENSILE BOND TESTING

Figure 41 - Tensile bond testing with Instron Tensile meter